Genome Assembly of Synthetic Allotetraploid *Brassica napus* Reveals Homoeologous Exchanges between Subgenomes

John T. Davis[*], Ruijuan Li[*†], Seungmo Kim[‡], Richard Michelmore[§], Shinje Kim[‡], Julin N. Maloof[*]

[*] Department of Plant Biology, University of California, Davis, Davis, CA, 95616

[†] Current Address: Inari Agriculture, Cambridge, MA

[‡] FnP Co., Ltd., Jeungpyeong, South Korea

[§] Genome Center and Department of Plant Sciences, University of California, Davis, Davis, CA, 95616

Running Title: Synthetic *B. napus* Genome Assembly

Keywords: Illumina, Dovetail, scaffolds, allotetraploid, subgenome

Corresponding authors:

Shinje Kim

Fungi and Plants, Corp.

60 Noam-ro, Doan-myeon

Jeungpyeong-gun, Chungbuk-do 27903

South Korea

sjekim@fnpco.com

+82-43-836-1751(tel)

Julin N Maloof

Department of Plant Biology

University of California, Davis

1 Shields Ave,

Davis, CA 95616

jnmaloof@ucdavis.edu

+1 (530) 752-8077

Abstract

Brassica napus, a globally important oilseed crop, is an allotetraploid hybrid species with two subgenomes originating from *B. rapa* and *B. oleracea.* The presence of two highly similar subgenomes has made the assembly of a complete draft genome challenging. The high degree of similarity between the subgenomes increases the difficulty of resolving the two subgenomes; it has also resulted in homoeologous exchanges between the genomes resulting in variations in gene copy number, which further complicates assigning sequences to correct chromosomes. Despite these challenges, high quality draft genomes of this species have been released; however, due to limitations of the contemporary sequencing technologies, these draft assemblies were not able to fully capture the genomic intricacies of this species. Using third generation sequencing and assembly technologies, we generated a new genome assembly for a synthetic *Brassica napus* cultivar, Da-Ae. Through the use of long reads, linked-reads, and Hi-C proximity data, we assembled a new draft genome that increases the assembly length of unambiguous bases by 47.5% in 19 chromosomal pseudomolecules relative to the current community genome reference and provides the community with a more complete reference genome of *Brassica napus*. In addition, we identified potential hotspots of homoeologous exchange between subgenomes within Da-Ae, based on their presence in other independently-derived lines. The occurrence of these hotspots may provide insight into understanding the genetic rearrangements required for *B. napus* to be viable following the hybridization of *B. rapa* and *B. oleracea.*

Introduction

Brassica napus, commonly known as rapeseed, is the second most widely cultivated oilseed crop in the world ("FAOSTAT", 2018). Historically, rapeseed oil was used primarily in the production of lubricants due to its high erucic acid content. In the late 1970s, new, edible, low erucic acid cultivars were created, enabling rapeseed oil to become a major component of most commercial vegetable oil products (Oplinger *et al.* 1989). The demand for rapeseed oil has caused global production to more than triple in the last few decades, with China and Canada being the world's largest producers ("PSD Online", 2018). Numerous attempts are being made to understand the biology of *B. napus* with the goal of increasing production to keep up with demand.

The genetics of *B. napus* is challenging to untangle due to its genomic complexity. *B. napus* is an outcrossing species that originated from the hybridization of two different diploid parents, *B. rapa* and *B. oleracea* (Nagaharu 1935). Both *B. rapa* and *B. oleracea* are widely cultivated as human food crops such as cabbage, bok choy, and broccoli. It is believed that *B. napus* first appeared approximately 7,500 years ago when *B. rapa* hybridized with *B. oleracea* and underwent a chromosome doubling event, resulting in an allotetraploid (Chalhoub *et al.* 2014). *B. napus* (AACC) contains the diploid genomes of both *B. rapa* (AA) and *B. oleracea* (CC). While polyploidy has been hypothesized to provide plants with advantages, such as favorability in domestication (Bertioli *et al.* 2019), it also has genetic consequences that can cause several analytical challenges. In the case of *B. napus*, the A and C subgenomes are so similar that there can be homoeologous exchange of genetic information between the two subgenomes. Such exchanges range in size from a few base pairs (gene conversion) to larger chromosomal regions

(Chalhoub *et al.* 2014). The rate and specifics of homoeologous exchange varies between *B. napus* populations and has been reported to occur more often in populations that have a newly synthesized *B. napus* as a parent (Udall *et al.* 2005). The exact mechanisms of this process are still unknown; however, the process is thought to be a driving factor in the large amount of diversity found within *B. napus*. Consequently, it has been challenging to generate a standard public consensus genome assembly for *B. napus*.

In 2014, a high-quality genomic reference assembly for *B. napus* was released to the public (Chalhoub *et al.* 2014). This assembly, hereby referred to as Darmor-bzh, was generated using short read sequencing data. Due to challenges associated with assembling and scaffolding short reads and the high similarity between the two subgenomes, a significant portion of the genome could not be confidently anchored in the assembly and was left unscaffolded. Since the release of the Darmor-bzh assembly, new sequencing and assembly strategies, including long reads, linked-reads, and proximity data, have become available and fiscally feasible. Recently new *B. napus* genomes using these technologies have been released to the public (Song *et al.* 2020). Concurrently we have generated a new genomic reference for a synthetic *B. napus* that includes a significant number of previously unscaffolded sequences. Additionally, this new assembly reveals shared and unique homoeologous exchange events in different *B. napus* lines.

Methods and Materials

Creation of Synthetic Brassica napus (Da-Ae)

The synthetic *B. napus* genotype Da-Ae (AACC, Korea patent number: 10-1432278-0000, 2014.08.13) was the focus of this study. Da-Ae was developed at FnPCo (South Korea) by

crossing an inbred *B. rapa (*AA) Chinese cabbage (WC720) with an inbred *B. oleracea (*CC) red cabbage (BW716). After hybridization, the F1underwent spontaneous chromosome doubling producing a naturally occurring allotetraploid *B. napus (*AACC). The hybrid was self-fertilized, and seven seeds were obtained and planted. Only three of the seven plants germinated and flowered, with only one producing seeds. Progeny from this plant were then self-fertilized for six generations with the final generation being designated Da-Ae.

Plant materials, DNA extraction, and library preparation

Three plant lines were sequenced in this study: the highly inbred Da-Ae, the male parent *B. rapa* (AA, WC720), and female parent *B. oleracea* (CC, BW716). For each line, 100 seeds from a single plant were germinated and grown for 8 to 10 days. The resulting seedlings were pooled separately for each line and high molecular weight genomic DNA extracted by Amplicon Express (Amplicon Express Inc., Pullman, WA, US). The quality of the DNA collected from these three samples was assessed using a Bioanalyzer (Agilent Technologies, Inc. Santa Clara, CA, US). A 10X Genomics library was prepared by the University of California, Davis (UCD) Genome Center. The resulting libraries were sequenced on an Illumina HiSeq X10 by Novogene (Novogene Corporation Inc., Sacramento, CA, US) as 150 bp paired-end reads producing ~451 million, ~380 million, and ~380 million reads for Da-Ae, the male parent, and the female parent, respectively. An additional 10X Genomics library for Da-Ae was constructed by the UCD Genome Center using a library prep involving sonication instead of the 10X Genomics' suggested library prep without sonication. This library was then sequenced on a HiSeq 4000 at the UCD Genome Center producing ~347 million 151 bp paired-end reads. For Pacific Biosciences (PacBio) sequencing, 32.9 µg high molecular weight DNA from Da-Ae was used for library construction

and 19 SMRTcells were sequenced on a PacBio Sequel system (Pacific Biosciences, Menlo Park, CA, US) at the UCD Genome Center, producing ~6.6 million subreads with an average length of ~11.2 Kb. An additional 100 seeds from the same single Da-Ae plant were grown to produce 4.5 g young leaf tissues that were sent to Dovetail Genomics (Dovetail Genomics, Scotts Valley, CA, US) for Hi-C library construction. The Hi-C library was then sequenced at the UCD Genome Center on an Illumina HiSeq 4000 producing ~374 million 150-bp paired-end reads.

Generation of 10X Genomics Assemblies

Initial assemblies of *B. napus* were generated using the default Supernova v1.1.5 pipeline (Weisenfeld *et al.* 2017) with an estimated genome size of 1.12 Gb. The 10X Genomics Da-Ae reads sequenced at the UCD Genome Center and Novogene (hereafter referred to as Da-Ae 10X Davis and Da-Ae 10X Novogene) were both assembled. The Da-Ae 10X Davis and Da-Ae 10X Novogene reads were arbitrarily split in half creating four sets of reads with coverage ranging from 40–60X, following the guidelines from 10X Genomics for using 36X–56X coverage when using Supernova. The four sets of reads were then assembled independently. All four assemblies had similar assembly statistics with both N_{50} (~140 Kb; Table 1) and total assembly lengths (793–806 Mb; Table 1) being lower than expected. Assemblies were completed again upon the release of Supernova-2.0.0. The 10X *B. rapa,* 10X *B. oleracea*, and 10X Da-Ae Davis reads were used in this round of assembly. The 10X Da-Ae Novogene reads were excluded due to having near identical assembly performance when compared to the 10X Da-Ae Davis reads. For the assemblies generated with Supernova-2.0.0, the reads sets were not arbitrarily split. Instead, the number of reads required for 56X coverage was calculated using the formula genome size x 56 / read length. The expected genome sizes used for *B. napus*, *B. rapa*, and *B.*

oleracea were 1.12 Gb, 530 Mb, and 630 Mb, respectively. These values were then input to Supernova-2.0.0 using the --maxreads parameter. Scaffolds from the three new Supernova assemblies were later used to assess mis-assemblies in Dovetail scaffolding based assemblies.

Generation of Pac-Bio Assemblies

The PacBio reads were assembled using two independent pipelines. PacBio's Falcon/Falcon_unzip pipeline (Chin *et al.* 2016) was the first pipeline used. Falcon and Falcon_unzip were installed under FALCON-integrate v.1.8.8. Falcon was run using the reference fc_run_plant configuration file that was modified for the 1.12 Gb genome size of *B. napus* and configured to run on a slurm controlled compute cluster. Upon completion, the assembly was phased using Falcon_unzip and the reference fc_unzip configuration file that was modified to run on a slurm controlled compute cluster. The phased assembly was then polished for one round using fc_quiver.py and the previously used fc_unzip configuration file.

Canu version 1.6 (Koren *et al.* 2017) from Maryland Bioinformatics Labs was the second pipeline used. Canu was configured for the 1.12 Gb genome size of *B. napus* and the reference suggestions for high coverage and polyploid organisms of corrected ErrorRate=0.040 and corOutCoverage=200. The Canu pipeline consisted of three separate steps: correction, trimming, and assembly.

Polishing of Pac-Bio Assemblies

Polishing was performed to improve the quality of both the Falcon/Falcon_unzip and Canu assemblies. Polishing was completed using the 10X Da-Ae Davis reads and the Broad Institute's program Pilon v.1.22 (Walker *et al.* 2014). Following the guidelines from 10X

Genomics, 23 bp of the start of read 1 and the first base pair of read 2 were removed using Trimmomatic v.0.33 (Bolger *et al.* 2014) in order to remove the 10X barcodes and frequently low-quality sequence. The trimmed reads were then mapped separately to both the Falcon/Falcon_unzip and Canu assemblies using bwa version 0.7.16a (Li and Durbin 2009). The two assemblies and the mapped read files were fed into Pilon. After polishing, both assemblies had approximately the same size and N_{50} as their unpolished counterparts.

Hi-C Scaffolding of Pac-Bio Assemblies

First, we chose the best Falcon and Canu assemblies based on N_{50}, assembly size, number of contigs, and benchmarking using universal single-copy ortholog (BUSCO) scores (Simão *et al.* 2015; Waterhouse *et al.* 2018). BUSCO scores were computed using BUSCOv3 and the Embryophyta odb9 dataset (Seppey *et al.* 2019). Then, these assemblies along with the Hi-C reads sequenced at the UCD Genome Center were sent to Dovetail Genomics for scaffolding. Both assemblies along with the Hi-C reads were run through Dovetail's proprietary HiRise pipeline where the individual contigs were scaffolded to create chromosome scale scaffolds.

Analysis of Hi-C Results

The N_{50}, assembly size, and BUSCO scores of both HiRise scaffolded assemblies were measured. The two HiRise generated assemblies were aligned to each other, using Nucmer from the MUMmer-3.23 bioinformatics package (Kurtz *et al.* 2004), and all scaffolds greater than 1 Mb were inspected to determine consensus between the two assemblies. Next, all scaffolds from the two HiRise generated assemblies were compared to the chromosomes of the publicly available Darmor-bzh genome (*B. napus* genome v4.1) hosted by the Brassica database

(BRAD) (Cheng *et al.* 2011). The scaffolds from each HiRise generated assembly were independently aligned to the Darmor-bzh chromosomes using Nucmer with the parameters --maxmatch -l 100 -c 500. The alignments were filtered for quality and all scaffolds were plotted (Figures 1–3). If a scaffold aligned best to one reference chromosome, it was assigned a name based on its alignment. All remaining scaffolds in each assembly were not renamed and retained their HiRise designated sequence IDs. Because the Canu assembly had a larger N50, a larger number of bases incorporated, more complete BUSCOs, and longer alignments with the current reference pseudomolecules, analysis was paused for the Falcon assembly and further analysis was continued for the Canu assembly.

Assessing Discrepancies between the Canu Assembly and the Public Reference Assembly

The 21 largest scaffolds in the Canu assembly were independently compared to their corresponding Darmor-bzh chromosomes. Regions of discrepancy between the Canu assembly and the reference assembly were identified. The validity of each discrepancy was then tested by aligning PacBio reads and 10X ancestral parent scaffolds to the Canu assembly. The PacBio reads were aligned using BLASR (Chaisson and Tesler 2012) with a minimum subread length of 10 Kb. The 10X ancestral parent scaffolds were aligned using Nucmer. If the region of discrepancy in the Canu assembly had significant support from the mapped reads and scaffolds, the discrepancy was considered a true difference between our assembly and the Darmor-bzh assembly and retained. If there was no support, or the mapped reads and scaffolds disagreed with the Canu assembly, the region of discrepancy was considered a likely error and altered to match Darmor-bzh. All alterations performed were simple sequence flips to fix assembly inversions. All inversions, except one, were almost exactly encapsulated within the contig

boundaries of a scaffold. After all identified discrepancies had been addressed, the assembly was considered final and annotation began (Figure 4, Supplementary Table 1).

Transcriptome Assembly and Structural Annotation of Novel Transcripts

RNA-seq reads from thirteen RNA sequencing libraries generated from five tissues (young leaf, flower, bolting tissue, 1 cm silique, and 5 cm silique) of Da-Ae (Li *et al.* 2018) were used for transcriptome assembly and annotation. The raw sequencing data were preprocessed and mapped to the published genome sequence of Darmor-bzh (*Brassica napus* genome v4.1) as described in Li et al., (2018). The mapped reads were then assembled by Cufflinks v2.2.1 (Trapnell *et al.* 2010) to transcripts with the help of reference annotations. The output GTF file generated by Cufflinks was fed to Cuffmerge and then Cuffcompare along with the annotations from the reference assembly. From the output file, transcripts with code "u" were considered novel. Redundant isoforms among these novel transcripts were removed using CAP3 (Huang and Madan 1999) and only transcripts with open reading frames detected using TransDecoder (Haas *et al.* 2013) were retained for the next step. For *de novo* assembly, post-processed high-quality reads were pooled together and assembled using Trinity (Grabherr *et al.* 2011) with default parameters. The abundance of transcripts was estimated using the Kallisto (Bray *et al.* 2016) method implemented in the Trinity pipeline, and those with less than 1 transcript per kilobase million were removed. Transcripts with detected open reading frames were aligned to the Darmor-bzh coding sequences (CDS) using BLASTN (AltschuP *et al.*) with an E-value cutoff of 1e-6, and those with high identity (≥ 95%) to Darmor-bzh CDS were filtered. An additional BLASTX search was conducted against NCBI non-redundant protein database using E-value 1e-6 to remove transcripts with no homology to known plant genes. The resulting assembly from

reference-based and *de novo* methods were combined for structural annotation using DAMMIT (Scott 2016) with default parameters to generate the final GFF3 file. BUSCO scores for the final assembly were calculated to assess transcriptome completeness.

Annotation using MAKER

Annotation was performed using MAKER v.3.01.02-beta (Cantarel *et al.* 2008; Campbell *et al.* 2014a). Prior to running the MAKER pipeline, a custom repeat library was constructed using the MAKER-P Repeat Library Construction-Advanced (Campbell *et al.* 2014b). Annotation using MAKER was run in two rounds. In order to speed up the annotation process, only the 19 named pseudomolecules were used and each pseudomolecule was annotated separately. In the first round of annotation, MAKER was run with the following parameters: The CDS transcripts from the Darmor-bzh assembly and the previously identified novel transcripts were used as expressed sequence tag (EST) evidence. The peptide sequences from *B. napus, B. oleracea,* and *B. rapa* downloaded from BRAD and the *A. thaliana* Araport11 peptides downloaded from the TAIR Project (Berardini *et al.* 2015) were used as evidence for protein homology. MAKER parameters that were modified included the following: Arabidopsis was used as the model species for Augustus; repeat library was set to the custom repeat library we constructed using the MAKER-P Repeat Library Construction-Advanced protocol; est2genome was set to 1; protein2genome was set to 1. All other parameters not stated above were left as the MAKER defaults. Due to an unresolved bioinformatic issue, 10 Kb of sequence of chrC01 starting at 47,446,387 had to be masked with N before MAKER would run to completion.

Upon completion of the first round of MAKER, the GFF files from each chromosome were concatenated. The GFF annotations were then filtered using Genome Annotation Generator (GAG) (Hall 2014) to remove questionable features. Following filtering, the annotations were then used to train SNAP (Korf 2004) using default parameters to generate an HMM file. Upon generation of the HMM file, the second round of MAKER was executed.

The second round of MAKER included all the scaffolds and used the same repeat library along with the same protein and EST evidence. est2genome and protein2genome were both set to 0 and snaphmm used the previously generated HMM file. Unlike the first round of annotation, Da-Ae was used as the model species for Augustus, and the Da-Ae model species files were generated through BUSCO using the long parameter. Once annotation of each chromosome was completed, the MAKER proteins were compared to the Uniref90 protein set using BLASTP. Protein domains were then identified using InterProScan on the MAKER predicted proteins. Using accessory scripts provided with MAKER, the MAKER genes were then renamed with the prefix “Bna” and the BLASTP and InterProScan results were integrated into the GFF annotation files. Finally, the annotations were filtered to remove any annotation that contained an Annotation Edit Distance (AED) score greater than 0.5. The cutoff of 0.5 was selected based on the recommendation listed in Campbell *et al*. (2014a).

Analysis of Homoeologous Exchange between Subgenomes

Homoeologous exchange is the exchange of genetic material from one subgenome to the other. This could result in the conversion of an A subgenome gene to a C subgenome gene or vice versa. Homoeologous exchange was explored using both gene and sequence level

analyses. Gene-level pairwise alignments between diploid genomes of Da-Ae, Darmor-bzh, Tapidor, *B. rapa,* and *B. oleracea* were made using JCVI's MCscan pipeline ("jcvi: JCVI utility libraries | Zenodo"). Complete conversions are events where both sister chromatids for a region in one subgenome are converted to the homoeologous version from the other subgenome but without a reciprocal exchange. As a result, the ratio of A:C or C:A at these homoeologous regions will become 4:0. By this criteria, homoeologous exchange was examined at both gene and sequence level contexts using genome and transcriptome information from Da-Ae, Darmor-bzh, *B. rapa, B. oleracea*, and an additional *B. napus* cultivar Tapidor (Bayer *et al.* 2017). Because our current assembly is unphased, attempting to identify potential 3:1 homoeologous ratios is inhibited by the assembler program creating a consensus sequence by either selecting one of the two homoeologous regions or creating a mashup of the two regions. In either case, the true underlying sequences are not being accurately represented by the assembly sequence. Thus, only complete conversions were explored.

To look for homoeologous exchange at the gene level, annotations of Da-Ae, Darmor-bzh, *B. rapa,* and *B. oleracea*, and an additional *B. napus* cultivar Tapidor, were used. CDS sequences for each gene were generated by gffread (Trapnell *et al.* 2010) using each assembly's GFF and sequence files. GFF annotations were converted to BED format using JCVI's jcvi.formats.gff module ("jcvi: JCVI utility libraries | Zenodo"). These BED files along with their corresponding CDS sequences were used as input for the MCscan pipeline of JCVI. Prior to running the MCscan pipeline, the *B. napus* CDS and BED files were separated into their two subgenomes, A and C, creating a CDS and BED file for both the A and C subgenomes. For each *B. napus* genome, the MCscan pipeline was run five times corresponding to five different pairwise

298 synteny searches*, B. rapa vs. B. napus A, B. rapa vs. B. napus C, B. oleracea vs. B. napus A, B.*
299 *oleracea vs. B. napus C,* and *B. napus A vs. B. napus C (*A_r-A_n, A_r-C_n, C_o-A_n, C_o-C_n, and A_n-C_n) with
300 a cscore filter of ≥ 0.99 to identify the reciprocal best hit (RBH) of each gene. *B. rapa* and *B.*
301 *oleracea* (A_r- C_o) were also aligned to one another for a total of 16 alignments. Although using a
302 cscore cutoff of 0.99 should return only RBHs, it is still possible for a tie to occur between
303 multiple query and subject sequences. If a tie occurred, the alignments were filtered to contain
304 the alignment that had the highest bit score. The resulting alignments were then analyzed in R
305 (R Core Team 2020) to identify potential genes that may have been involved in homoeologous
306 exchange. For simplicity of analysis, RBH gene alignments between *B. rapa* and *B. oleracea*
307 were used to filter potential genes involved in homoeologous exchange between the A and C
308 subgenomes of *B. napus*. A homoeologous gene pair was considered a possible site of
309 homoeologous exchange if two requirements were met. First, one gene of the pair must align
310 better to its homoeolog than it does to its ortholog. Second, the gene must also align better to
311 its homoeolog's ortholog than it does to its own ortholog. For example, consider the case of a
312 gene on the *B. napus* C subgenome being converted to the *B. napus* A subgenome form. The
313 gene in the C subgenome will align better to its homoeolog in the A subgenome than to its
314 ortholog in the *B. oleracea* genome. The gene in the C subgenome will also align better to its
315 homoeolog's ortholog in the *B. rapa* genome than to its ortholog in the *B. oleracea* genome
316 (Figure 5). However, if an annotation is incomplete or erroneous, it can create both false
317 positive and false negative results.

318 For sequence level analysis of homoeologous exchange, the barcode removed 10X Da-
319 Ae Davis reads, genomic reads from Darmor-bzh, and genomic reads from Tapidor were used.

All reads were trimmed for quality using Trimmomatic and the adapter sequences with the parameters ILLUMINACLIP:adapters.fa:2:30:10 LEADING:3 TRAILING:3 SLIDINGWINDOW:4:15 MINLEN:36 before being mapped with BWA to an *in silico B. napus* genome constructed by combining both the *B. rapa* (Cheng *et al.* 2013) and the *B. oleracea* (Liu *et al.* 2014) chromosomes. To find possible sites of homoeologous exchange, we first filtered reads to retain those that could reliably be described as coming from either the A or C subgenome (i.e., those with unique and trustworthy mapping locations). To do so, the alignment files were filtered to only contain alignments that had a MAPQ of five or greater, were properly paired, had no supplementary alignments, and were primary alignments. Reads from these alignments were then mapped to their source genomes and filtered for alignments with a MAPQ of five or greater. bedcov from Samtools (Li *et al.* 2009) was then used to calculate the coverage across the genomes and the coverage of the individual potential genes previously identified. To calculate coverage across the genomes, a window size of 100 Kb with a step size of 20 Kb was used. The calculated coverages were standardized based on the chromosome using R (R Core Team 2020). Prior to standardization, regions that contained ≥10X mean coverage of their chromosome were removed from further analysis. The coverages were then plotted to identify regions across the genome with higher or lower than average coverage. These regions were considered potential sites of homoeologous exchange. The coverage of the potential homoeologous genes was also compared to the genome coverage to look for agreement between the two methods.

Analysis of Genome Completeness

To look at the completeness of each of the Da-Ae and Darmor-bzh genomes, a Unigene set of 133,127 *Brassica* sequences (http://www.brassica.info/resource/transcriptomics/BrasEX1s.unigene.public.fasta) was aligned to each genome using BLASTN with a E-value cutoff of 1e-3. Following alignment, hits were defined as those with a 90% or greater identity. The *Brassica* Unigene sequences present in one genome but not the other were used for follow-up analysis. Each *Brassica* unigene sequence was assigned predicted GO terms using *Arabidopsis thaliana* GO terms (ftp://ftp.arabidopsis.org/home/tair/Ontologies/Gene_Ontology/ATH_GO_GOSLIM.txt) along with BLASTN alignments of the *Brassica* Unigene sequences to identify homologous *A. thaliana* genes (http://www.brassica.info/resource/transcriptomics/BrasEx1s.unigene_v_at.1e-5.tophit.txt). If a sequence did not have an alignment to *A. thaliana* or was missing GO term definitions, it was dropped from the set. The *Brassica* Unigene sequences with their added GO terms were then analyzed for GO term enrichment in R (R Core Team 2020) using the "goseq" package (Young *et al.* 2010). Sequences present in one genome but not the other were analyzed to look for GO term enrichment by using all the sequences present in Da-Ae and Darmor-bzh as the universe and sequences unique to one genome as the target. The GO terms deemed to be over-represented using a p-value cutoff of 0.05 were then visualized using Revigo (Supek *et al.* 2011).

Data Availability

All sequencing data produced in this study can be found under the BioProject PRJNA627442 (Reviewer link https://dataview.ncbi.nlm.nih.gov/object/PRJNA627442?reviewer=5o8tsi1ik3chr81pi6rfntae71;

will be made public upon paper acceptance). This Whole Genome Shotgun project has been deposited at DDBJ/ENA/GenBank under the accession JAGKQM000000000. The version described in this paper is version JAGKQM010000000. Darmor-bzh, *Brassica rapa*, and *Brassica oleracea* genomes and annotations were retrieved from the publicly available BRAD database (http://brassicadb.org/brad/). Genome sequences and annotations of Tapidor were retrieved from Applied Bioinformatics Group site (http://appliedbioinformatics.com.au/index.php/Darmor_Tapidor). *Arabidopsis thaliana* Araport 11 annotations were retrieved from the TAIR project (https://www.arabidopsis.org/).

Code availability

Scripts used in this analysis are available at https://github.com/MaloofLab/Davis_B_napus_assembly_2021.

Results

To develop a high-quality, more complete assembly of *B. napus* we took advantage of contemporary technologies by using a combination of 10X Genomics, Pacific Biosciences, and Dovetail / Hi-C methods (Figure 6). The application of each is described in turn below, followed by the results of the annotation and homoeologous exchange analysis.

Supernova assemblies

The first assembly attempts were made using 10X Da-Ae Davis and 10X Da-Ae Novogene reads along with the default Supernova-1.1.5 pipeline and an estimated genome size of 1.12 Gb. A total of four pseudohap assembly files, two from 10X Da-Ae Davis and two from 10X Da-

Ae Novogene, were created (see methods). The assembly lengths ranged from 793–806 Mb with an average size of 801 Mb and the N_{50}s ranged from 140–150 Kb with an average size of 143 Kb. All assemblies had approximately 80,000 scaffolds (Table 1) and poor BUSCO scores for the number of complete BUSCOs and proportion of single to duplicate BUSCOs when compared to the public reference (Table 1). Given that *B. napus* is a recent allotetraploid, one would expect to see a higher number of duplicate BUSCO genes due to a copy being present in both subgenomes. It is not standard procedure when generating 10X libraries to perform fragmentation using sonication, but given the highly similar assembly results, it suggests that the method of fragmentation did not alter assembly performance. Following the release of Supernova v2.0.0, the 10X Da-Ae Davis reads were reassembled. The new assembly had a length of 918 Mb and an N_{50} of 1.5 Mb. Additionally, the number of scaffolds was halved to ~36,000 (Table 1). Notably, the BUSCO scores of this new assembly greatly improved, approaching the scores of the Darmor-bzh (Table 1). The 10X reads for both *B. rapa* and *B. oleracea* assembled using Supernova v2.0.0 also showed promising results. Both assemblies had N_{50} values over 2 Mb and consisted of less than 20,000 scaffolds (Table 1). Although all assemblies were smaller than the expected genome sizes, they were all on par with the sizes of the public references. The assembly metrics and BUSCO scores encouraged the use of the assembly scaffolds in the manual curation of future assemblies.

PacBio assemblies

Two different long read assemblers were used in this project, Falcon and Canu. The initial Canu assembly was both larger and had better BUSCO scores than the initial unphased Falcon assembly; however, the Canu assembly also had twice the number of contigs and a

modestly lower N_{50} compared to the Falcon assembly (Table 1). The initial Falcon assembly was substantially improved after phasing using the Falcon_unzip pipeline. The phasing pipeline created a primary haplotig assembly, which while smaller in size than the input assembly, had a larger N_{50}, fewer contigs, and a slight increase in BUSCO scores. Improvement continued after one round of polishing using Quiver from the Falcon_unzip pipeline. Following Quiver polishing, the Falcon assembly had a larger assembly size and N_{50} than its unpolished counterpart. Additionally, the number of contigs decreased again and the Falcon assembly now had a larger number of complete BUSCOs compared to the Canu assembly (Table 1). With the assembly pipeline of both assemblers complete, additional polishing was completed using Pilon and the 10X Da-Ae reads. After polishing with Pilon, the Canu assembly had a larger N_{50}, smaller assembly size, and more complete BUSCOs compared to its unpolished counterpart. Likewise, the Falcon assembly had a smaller N_{50}, smaller assembly size, and same number of complete BUSCOs compared to its unpolished form. Both the Canu and Falcon assemblies had similar BUSCO scores, but different N_{50}, size, and contig numbers.

Dovetail Scaffolding

Based upon the assembly metrics and BUSCO scores, the Pilon-polished Canu and Quiver-polished Falcon assemblies, as well as the previously sequenced Hi-C reads, were selected for scaffolding using the HiRise pipeline by Dovetail Genomics. After HiRise scaffolding, the Canu and Falcon assemblies showed large increases in N_{50} from 1.59 Mb to 42.79 Mb and from 1.80 Mb to 35.52 Mb, respectively. The Canu assembly was now composed of 3,190 scaffolds and the Falcon assembly had 709 scaffolds (Table 1). The Canu and Falcon assemblies also had 23 and 29 scaffolds greater than 1 Mb, respectively, with the largest being 74.2 Mb.

The scaffolds from each assembly were aligned against each other using Nucmer. Looking at the resulting plot (Figure 1), the scaffolds are highly collinear except for one region where two scaffolds have an inversion relative to each other. In several cases, it took two Falcon scaffolds to span one Canu scaffold, suggesting that HiRise was better able to scaffold the Canu assembly than the Falcon assembly. Regarding BUSCO scores, the scaffolding caused the single to duplicate ratio to increase in the Falcon assembly and decrease in the Canu assembly, resulting in an increase in the number of complete BUSCOs in the Canu assembly (Table 1).

Assigning Scaffolds to Chromosomes

To assign the scaffolds to the established chromosomes, the two assemblies were aligned to the Darmor-bzh assembly using Nucmer. The 19 Darmor-bzh chromosomes were covered by the 21 largest Canu scaffolds; 17 spanned the full length of their sister Darmor-bzh scaffold while the remaining four scaffolds had to be concatenated in pairs to span ChrC06 and ChrC07 (Figure 2). The 27 largest Falcon scaffolds spanned all 19 chromosomes with two Falcon scaffolds needing to be concatenated to span each of multiple Darmor-bzh chromosomes (Figure 3). Names were then assigned to the scaffolds based on which Darmor-bzh chromosome they aligned to.

Assembly Discrepancies

After the scaffolds of each assembly had been assigned to chromosomes, the Canu assembly was selected for further analysis based on its better overall size, N_{50}, contiguity, alignment to Darmor-bzh, and BUSCO scores. Comparison of the Canu assembly to the Darmor-bzh assembly revealed 24 assembly discrepancies (Supplemental Table 1). These discrepancies

included inversions, lack of contiguity, and introduction of new sequence. To assess the validity of these discrepancies, both the parental 10X scaffolds and the PacBio reads were mapped to the Canu assembly. In 15 of the 24 discrepancies, the Canu assembly was supported by either read mapping or scaffold evidence. In ChrC06 and ChrC07, two scaffolds spanned the whole reference chromosome but failed to be scaffolded together. These scaffolds were joined with 100 Ns to signify a scaffolding gap and were then able to span the entire Darmor-bzh chromosome as one scaffold. In six cases, the Canu assembly had unsupported inversions with four of the inversions spanning from one scaffold gap to another scaffold gap. For each case, the sequence was inverted to match the Darmor-bzh assembly. The most prominent discrepancy occurred on ChrA05. Alignment to Darmor-bzh suggested that both chromosome arms were inverted at their junction with the centromere. As there was no read or scaffolding evidence to support this, both chromosome arms were inverted to match Darmor-bzh. Although our chrA05 now agrees with the Darmor-bzh assembly, the orientation and centromeric region remains questionable. After all discrepancies were addressed, the assembly was deemed final and annotation began (Figure 4).

Annotation

MAKER analysis of the Da-Ae assembly predicted 96,442 protein coding genes after filtering, compared to the 101,400 genes annotated in the reference assembly. To explore these differences, we determined the location of the predicted genes in their respective assemblies. While Da-Ae contains fewer gene models than Darmor-bzh, 88,605 of the Da-Ae gene models are present on its 19 pseudomolecules compared to Darmor-bzh, which contains

80,927 gene models on its 19 pseudomolecules (Table 1). This indicates the improved assembly of pseudomolecules in the Da-Ae assembly.

To further explore the discrepancy in annotated gene number, we determined how much of the discrepancy was due to differences in annotation versus differences in assembly. Of the 101,040 predicted Darmor-bzh genes, 100,575 are present in the Da-Ae genome assembly and 91,949 are present in the Da-Ae predicted gene set (8,626 Darmor-bzh predicted genes are present in the Da-Ae assembly but not annotated as genes). Similarly, of the 96,442 predicted Da-Ae genes, 95,991 are present in the Darmor-bzh genome assembly and 88,303 are present in the Darmor-bzh predicted gene set (7,688 Da-Ae predicted genes are present in the Darmor-bzh assembly but not annotated as genes). Thus, almost all of the genes predicted from one genome are present in the other genome, but 8–8.5% of the predicted genes from one genome were not annotated in the other genome. One possible explanation for genes that are only present in one of the two annotations is that they are not true genes. Indeed, while the average length of predicted Darmor-bzh genes that have a match among Da-Ae predicted gene is 1,048 bases, those that are present in the Da-Ae genome but missing from the Da-Ae annotation average only 536 bases in length. Thus, much of the discrepancy in annotation is due to small predicted gene products that may not be true genes or are difficult to reliably annotate.

Final Assembly Comparison

The final Da-Ae assembly improves upon the Darmor-bzh assembly by a number of criteria (Table 3). Comparing the full assemblies and the pseudomolecule assemblies,

respectively, the N50 is 24% to 32% longer, there are 36% to 47% more unambiguous bases incorporated into the Da-Ae assembly, and there are 1% to 4% more complete BUSCOs in the Da-Ae assembly. As for gene models, Da-Ae had 5% less than Darmor-bzh in the full assembly, but 9% more gene models incorporated into pseudomolecules.

Genome Completeness Analysis

Genome completeness of Da-Ae and Darmor-bzh was analyzed using the public Unigene set of 133,127 Brassica sequences. Of the 133,127 sequences, 117,447 (88.22%) were present in both genomes, 1,300 (0.98%) were present in only Da-Ae, 1,198 (0.90%) were present in only Darmor-bzh, and 13,182 (9.90%) were missing from both genomes. To determine there were particular classes of genes that were deleted in these genomes, we looked for enriched GO terms among the set of genes that were either present in Da-Ae and missing in Darmor-bzh or present in Darmor-bzh but missing in Da-Ae. We found an enrichment for genes involved in very long chain fatty acid metabolism, perhaps reflecting different breeding selection targets for these oil-seed crops (Figure 7). We also found enrichment for genes involved in several hormone pathways and in cuticle development, potentially representing adaptations to different environmental stressors (Figure 7).

Homoeologous Exchange

Homoeologous exchange is the exchange of genetic material from one subgenome to the other. This could result in the conversion of an A subgenome gene to a C subgenome gene or vice versa. *B. napus* is an allotetraploid containing two diploid subgenomes A and C, meaning homoeologous exchange can result in homoeolog ratios of 2:2, 3:1, or 4:0, corresponding to

reciprocal, partial, or complete conversions, respectively. For ease of detection given our unphased assembly we focused on complete conversions for our homoeologous exchange analysis.

At the gene level, there were 2,189, 1,848, and 823 potential gene pairs in Da-Ae, Darmor-bzh, and Tapidor where the C subgenome gene was a copy of the A subgenome gene. Conversely, there were 1,815, 1,666, and 666 potential gene pairs where the A subgenome gene was a copy of the C subgenome gene. To further validate these candidates, homoeologous exchange candidate gene pairs were next filtered based on their genomic sequencing coverage. If a C to A conversion has taken place, the expected average coverage ratio between orthologs should be 3:1 or greater when mapping reads to an *in silico* combined *B. rapa* + *B. oleracea* reference genome and should be 1:1 between homoeologs in the *B. napus* genome. Thus, a candidate exchange gene pair was retained if the ratio of coverage between the *B. rapa* and *B. oleracea* orthologs was at least 2.5 and the ratio of coverage between the two *B. napus* homeologs was between 0.5 and 1.5. After filtering, 234, 137, and 80 gene pairs remained in the C converted to A case, and 123, 150, and 31 in the A converted to C case for Da-Ae, Darmor-bzh, and Tapidor, respectively. Between the three *B. napus* genomes, only six C to A and one A to C gene conversions were shared (Figure 8). Interestingly, there was only one *B. rapa* to *B. oleracea* gene pair that showed opposite conversions between the Da-Ae and Darmor-bzh genome, where an A to C conversion took place in Da-Ae and a C to A conversion took place in Darmor-bzh.

At the sequence level, homoeologous exchange was examined by looking at the coverage across the genome using the previously described alignments. In regions where

533 homoeologous exchange has occurred, we would expect an increase in the coverage of reads
534 mapped to the donor region and a decrease in the coverage of reads mapped to the recipient
535 region in the *in silico B .rapa* + *B. oleraceae* combined genome. This is due to the *in silico*
536 recipient region being replaced with the donor region in the *B. napus* genome. In the *B.* napus
537 genome, there would be an equal increase in coverage for reads mapped to both
538 homoeologous exchange regions since both regions will be identical, allowing reads to map to
539 both regions equally well. We observed sites of possible homoeologous exchange on every
540 chromosome in the *B. napus* genome in regions ranging from 100 Kb to greater than 1 Mb.
541 There are several large regions that appear to have undergone homoeologous exchange in two
542 or more *B. napus* genomes (Figure 9). At the same time, each *B. napus* genome appears to
543 contain numerous smaller sites of homoeologous exchange that are unique to their genome
544 (Figure 10).

545 **Discussion**

546 Since the release of the first reference genome (Chalhoub *et al.* 2014), multiple research groups
547 have released genome assemblies of different *B. napus* cultivars, analyzed homoeologous
548 exchange, and identified quantitative trait loci (QTLs) related to key agricultural traits (Wang *et*
549 *al.* 2015, 2016; Bayer *et al.* 2017; Samans *et al.* 2017; Stein *et al.* 2017; Song *et al.* 2020). These
550 efforts all contribute to untangling the genome biology of *B. napus* that will one day be
551 combined to create a species-wide pangenome.

552 The original *B. napus* reference was assembled and released during a time when
553 sequencing technologies from PacBio, 10X Genomics, and Dovetail Genomics were in their

554 infancy and/or not fiscally feasible for most research groups. As a result, the first release of the
555 *B. napus* genome was not able to benefit from the analytical power of these technologies. This
556 is reflected in the assembly size of the Darmor-bzh genome (Chalhoub *et al.* 2014). Although
557 the expected size of the *B. napus* genome is over 1 Gb, the Darmor-bzh genome assembly is
558 only approximately 850 Mb of which 650 Mb is contained in 19 chromosome-scale
559 pseudomolecule scaffolds. By using a recently created synthetic *B. napus*, *Da-Ae*, along with
560 long-read, linked-read, and proximity ligation technologies, we were able to generate a new *B.*
561 *napus* genome reference that exceeded the previous high-quality reference genome by several
562 metrics. Our assembly of Da-Ae is over 1 Gb, with more than 800 Mb contained within 19
563 chromosome-scale pseudomolecule scaffolds. While our assembly is larger compared to the
564 Darmor-bzh assembly, it still maintains a high level of sequence collinearity with much of the
565 increase in length being due to sequences in the Darmor-bzh assembly that were not anchored
566 in the 19 chromosome pseudomolecules being included in the Da-Ae assembly. On a gene level,
567 the Darmor-bzh reference does have slightly more annotated genes than our assembly, but the
568 great majority of these are very small in length and most likely do not reflect true genes. While
569 Darmor-bzh has more annotated genes, our Da-Ae assembly has a higher number of gene
570 models located on the 19 pseudomolecules. The improved assembly enabled by third
571 generation sequencing technologies will serve as an excellent resource for *B. napus* geneticists
572 and scientists aiming to identify genes underlying agronomic traits.

573 Homoeologous exchange is a biological process observed in allopolyploids, like *B. napus*,
574 where highly similar yet different regions of the two diploid subgenomes exchange genetic
575 material with one another. The result is new chromosome structures that, while being primarily

composed of one ancestral genome, now also contain regions belonging to a different ancestral genome. To investigate the occurrence of homoeologous exchange in Da-Ae, we investigated both genome coverage and gene content across the genomes of three assemblies of *B. napus*, Da-Ae, Darmor-bzh, and Tapidor. Our results indicate that homoeologous exchange has occurred in both small and large regions throughout the whole genome. Each cultivar of *B. napus* had many unique homoeologous exchange events. More surprising was that there are multiple large regions of homoeologous exchange that are shared among the three *B. napus* cultivars. These shared regions may be homoeologous exchange hotspots for chromosomal rearrangements, which are required for viable *B. napus* cultivars to exist and further build upon the previous work done to identify hotspot regions (Higgins *et al.* 2018). Further investigation is needed to see how prevalent these shared homoeologous exchange regions are in the *B. napus* species.

In conclusion, using several recent sequencing technologies, we created a genome assembly that improves upon previous assemblies. We were able to include sequences that were previously unassigned, thus increasing the completeness of the *B. napus* genome assembly. We also identified potential hotspots of homoeologous exchange along with single-copy BUSCOs that are shared among different cultivars of *B. napus*. Our assembly and analysis of Da-Ae is another step forward toward the realization of a pangenome for *B. napus*.

Acknowledgements

We would like to thank the members of the Michelmore Lab (UC Davis), especially Kyle Fletcher, William Palmer, and Sebastian Reyes Chin Wo, for countless hours of advice and support throughout this project. This study was funded by a grant from the Korean Institute for Advancement of Technology (KIAT) along with additional funds from Fungi and Plants Corp. and University of California Davis (KIAT Project # N0001725), and a grant from Korea Institute of Planning and Evaluation for Technology in Food, Agriculture and Forestry (IPET project # 318023-04).

References

AltschuP, S. F., W. Gish, W. Miller, E. W. Myers, and D. J. Lipman Basic Local Alignment Search Tool. 8.

Bayer, P. E., B. Hurgobin, A. A. Golicz, C.-K. K. Chan, Y. Yuan *et al.*, 2017 Assembly and comparison of two closely related Brassica napus genomes. Plant Biotechnology Journal 15: 1602–1610.

Berardini, T. Z., L. Reiser, D. Li, Y. Mezheritsky, R. Muller *et al.*, 2015 The arabidopsis information resource: Making and mining the "gold standard" annotated reference plant genome. genesis 53: 474–485.

Bertioli, D. J., J. Jenkins, J. Clevenger, O. Dudchenko, D. Gao *et al.*, 2019 The genome sequence of segmental allotetraploid peanut Arachis hypogaea. Nat Genet 51: 877–884.

Bolger, A. M., M. Lohse, and B. Usadel, 2014 Trimmomatic: a flexible trimmer for Illumina sequence data. Bioinformatics 30: 2114–2120.

Bray, N. L., H. Pimentel, P. Melsted, and L. Pachter, 2016 Near-optimal probabilistic RNA-seq quantification. Nature Biotechnology 34: 525–527.

Campbell, M. S., C. Holt, B. Moore, and M. Yandell, 2014a Genome Annotation and Curation Using MAKER and MAKER-P: Genome Annotation and Curation Using MAKER and MAKER-P, pp. 4.11.1-4.11.39 in *Current Protocols in Bioinformatics*, edited by A. Bateman, W. R. Pearson, L. D. Stein, G. D. Stormo, and J. R. Yates. John Wiley & Sons, Inc., Hoboken, NJ, USA.

Campbell, M. S., M. Law, C. Holt, J. C. Stein, G. D. Moghe *et al.*, 2014b MAKER-P: A Tool Kit for the Rapid Creation, Management, and Quality Control of Plant Genome Annotations. PLANT PHYSIOLOGY 164: 513–524.

Cantarel, B. L., I. Korf, S. M. C. Robb, G. Parra, E. Ross *et al.*, 2008 MAKER: An easy-to-use annotation pipeline designed for emerging model organism genomes. Genome Res 18: 188–196.

Chaisson, M. J., and G. Tesler, 2012 Mapping single molecule sequencing reads using basic local alignment with successive refinement (BLASR): application and theory. BMC Bioinformatics 13: 238.

Chalhoub, B., F. Denoeud, S. Liu, I. A. P. Parkin, H. Tang *et al.*, 2014 Early allopolyploid evolution in the post-Neolithic Brassica napus oilseed genome. Science 345: 950–953.

Cheng, F., S. Liu, J. Wu, L. Fang, S. Sun *et al.*, 2011 BRAD, the genetics and genomics database for Brassica plants. BMC Plant Biology 11: 136.

Cheng, F., T. Mandáková, J. Wu, Q. Xie, M. A. Lysak *et al.*, 2013 Deciphering the Diploid Ancestral Genome of the Mesohexaploid *Brassica rapa*. The Plant Cell 25: 1541–1554.

Chin, C.-S., P. Peluso, F. J. Sedlazeck, M. Nattestad, G. T. Concepcion *et al.*, 2016 Phased diploid genome assembly with single-molecule real-time sequencing. Nature Methods 13: 1050–1054.

FAOSTAT.

Grabherr, M. G., B. J. Haas, M. Yassour, J. Z. Levin, D. A. Thompson *et al.*, 2011 Full-length transcriptome assembly from RNA-Seq data without a reference genome. Nature Biotechnology 29: 644–652.

Haas, B. J., A. Papanicolaou, M. Yassour, M. Grabherr, P. D. Blood *et al.*, 2013 De novo transcript sequence reconstruction from RNA-Seq: reference generation and analysis with Trinity. Nat Protoc 8:.

Hall, B., 2014 *GAG: the Genome Annotation Generator*.

Higgins, E. E., W. E. Clarke, E. C. Howell, S. J. Armstrong, and I. A. P. Parkin, 2018 Detecting de Novo Homoeologous Recombination Events in Cultivated Brassica napus Using a Genome-Wide SNP Array. G3 (Bethesda) 8: 2673–2683.

Huang, X., and A. Madan, 1999 CAP3: A DNA Sequence Assembly Program. Genome Res 9: 868–877.

jcvi: JCVI utility libraries | Zenodo.

Koren, S., B. P. Walenz, K. Berlin, J. R. Miller, N. H. Bergman *et al.*, 2017 Canu: scalable and accurate long-read assembly via adaptive *k* -mer weighting and repeat separation. Genome Research 27: 722–736.

Korf, I., 2004 Gene finding in novel genomes. BMC Bioinformatics 9.

Kurtz, S., A. Phillippy, A. L. Delcher, M. Smoot, M. Shumway *et al.*, 2004 Versatile and open software for comparing large genomes. Genome Biology 9.

Li, H., and R. Durbin, 2009 Fast and accurate short read alignment with Burrows–Wheeler transform. Bioinformatics 25: 1754–1760.

Li, H., B. Handsaker, A. Wysoker, T. Fennell, J. Ruan *et al.*, 2009 The Sequence Alignment/Map format and SAMtools. Bioinformatics 25: 2078–2079.

Li, R., K. Jeong, J. T. Davis, S. Kim, S. Lee *et al.*, 2018 Integrated QTL and eQTL Mapping Provides Insights and Candidate Genes for Fatty Acid Composition, Flowering Time, and Growth Traits in a F2 Population of a Novel Synthetic Allopolyploid Brassica napus. Front. Plant Sci. 9:.

Liu, S., Y. Liu, X. Yang, C. Tong, D. Edwards *et al.*, 2014 The Brassica oleracea genome reveals the asymmetrical evolution of polyploid genomes. Nat Commun 5: 3930.

Nagaharu, U., 1935 Genome Analysis in Brassica with Special Reference to the Experimental Formation of B. Napus and Peculiar Mode of Fertilization. Japanese Journal of Botany 389–452.

Oplinger, E. S., L. L. Hardman, E. T. Gritton, J. D. Doll, and K. Kelling, 1989 Canola (Rapeseed): Alternative Field Crops Manual. Collection: Alternative Field Crops Manual.

PSD Online.

R Core Team, 2013 *R: A language and environment for statistical computing.* R Foundation for Statistical Computing, Vienna, Austria.

Samans, B., B. Chalhoub, and R. J. Snowdon, 2017 Surviving a Genome Collision: Genomic Signatures of Allopolyploidization in the Recent Crop Species Brassica napus. The Plant Genome 10: plantgenome2017.02.0013.

Scott, C., 2016 dammit: an open and accessible de novo transcriptome annotator. in prep.

Seppey, M., P. Ioannidis, B. C. Emerson, C. Pitteloud, M. Robinson-Rechavi *et al.*, 2019 Genomic signatures accompanying the dietary shift to phytophagy in polyphagan beetles. Genome Biology 20: 98.

Simão, F. A., R. M. Waterhouse, P. Ioannidis, E. V. Kriventseva, and E. M. Zdobnov, 2015 BUSCO: assessing genome assembly and annotation completeness with single-copy orthologs. Bioinformatics 31: 3210–3212.

Song, J.-M., Z. Guan, J. Hu, C. Guo, Z. Yang *et al.*, 2020 Eight high-quality genomes reveal pan-genome architecture and ecotype differentiation of Brassica napus. Nature Plants 6: 34–45.

Stein, A., O. Coriton, M. Rousseau-Gueutin, B. Samans, S. V. Schiessl *et al.*, 2017 Mapping of homoeologous chromosome exchanges influencing quantitative trait variation in Brassica napus. Plant Biotechnology Journal 15: 1478–1489.

Supek, F., M. Bošnjak, N. Škunca, and T. Šmuc, 2011 REVIGO Summarizes and Visualizes Long Lists of Gene Ontology Terms. PLOS ONE 6: e21800.

Trapnell, C., B. A. Williams, G. Pertea, A. Mortazavi, G. Kwan *et al.*, 2010 Transcript assembly and quantification by RNA-Seq reveals unannotated transcripts and isoform switching during cell differentiation. Nat. Biotechnol. 28: 511–515.

Udall, J. A., P. A. Quijada, and T. C. Osborn, 2005 Detection of chromosomal rearrangements derived from homologous recombination in four mapping populations of Brassica napus L. Genetics 169: 967–979.

Walker, B. J., T. Abeel, T. Shea, M. Priest, A. Abouelliel *et al.*, 2014 Pilon: An Integrated Tool for Comprehensive Microbial Variant Detection and Genome Assembly Improvement (J. Wang, Ed.). PLoS ONE 9: e112963.

Wang, H., H. Cheng, W. Wang, J. Liu, M. Hao *et al.*, 2016 Identification of BnaYUCCA6 as a candidate gene for branch angle in Brassica napus by QTL-seq. Scientific Reports 6: 38493.

Wang, X., K. Yu, H. Li, Q. Peng, F. Chen *et al.*, 2015 High-Density SNP Map Construction and QTL Identification for the Apetalous Character in Brassica napus L. Front. Plant Sci. 6:.

Weisenfeld, N. I., V. Kumar, P. Shah, D. M. Church, and D. B. Jaffe, 2017 Direct determination of diploid genome sequences. Genome Res. 27: 757–767.

Young, M. D., M. J. Wakefield, G. K. Smyth, and A. Oshlack, 2010 Gene ontology analysis for RNA-seq: accounting for selection bias. Genome Biology 11: R14.

Figures

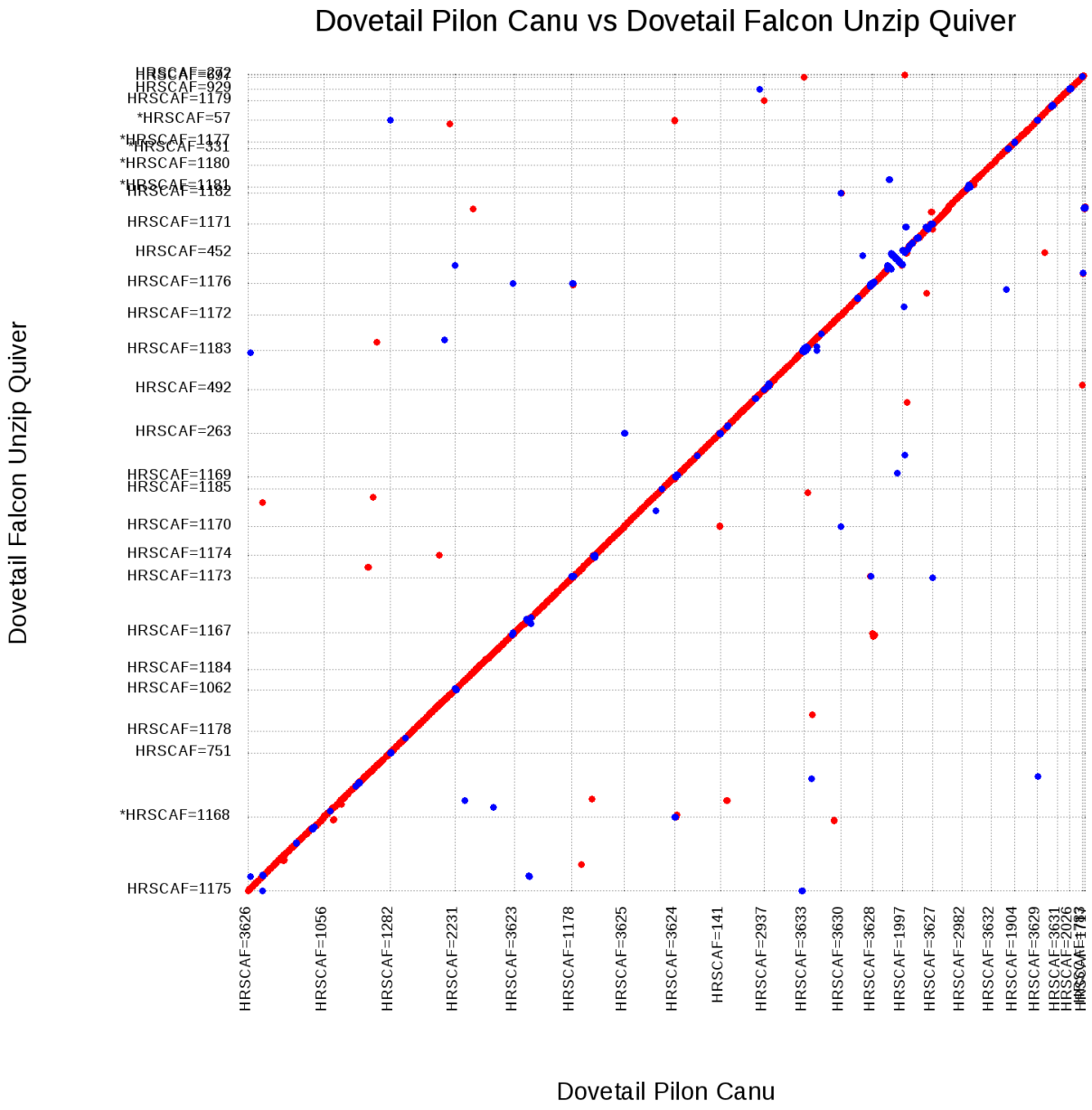

Figure 1 Nucmer plot of Dovetail_Falcon_Unzip_Quiver aligned to Dovetail_Pilon_Canu. All sequences aligned are 1 Mbp or greater. Red indicates an alignment in the forward direction and blue indicates an alignment in the reverse direction.

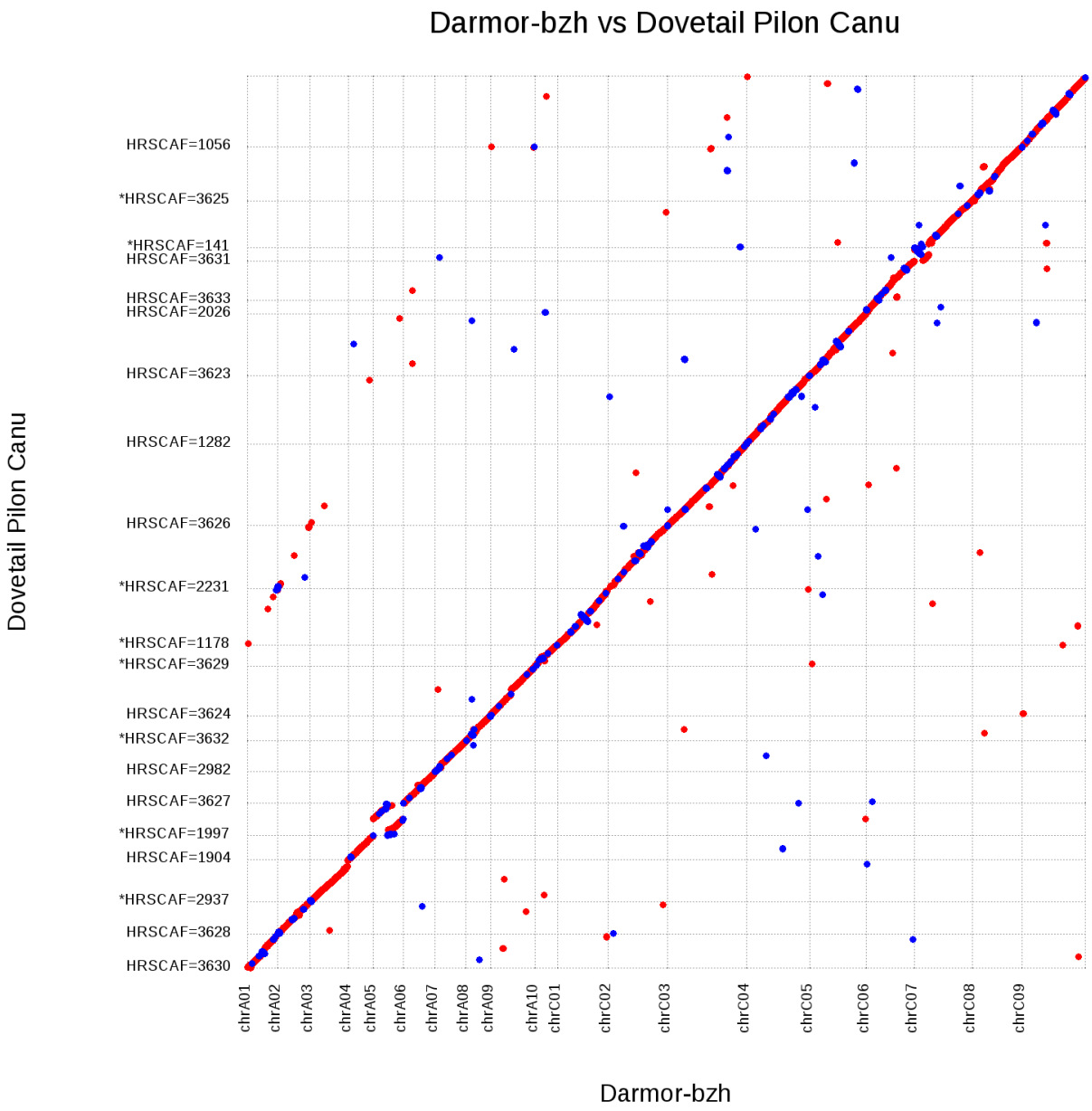

Figure 2 Nucmer plot of Dovetail_Pilon_Canu aligned to Darmor-bzh reference chromosomes. All sequences aligned are 1 Mbp or greater. A total of 21 Dovetail_Pilon_Canu scaffolds are aligned to 19 reference chromosomes. Red indicates an alignment in the forward direction and blue indicates an alignment in the reverse direction.

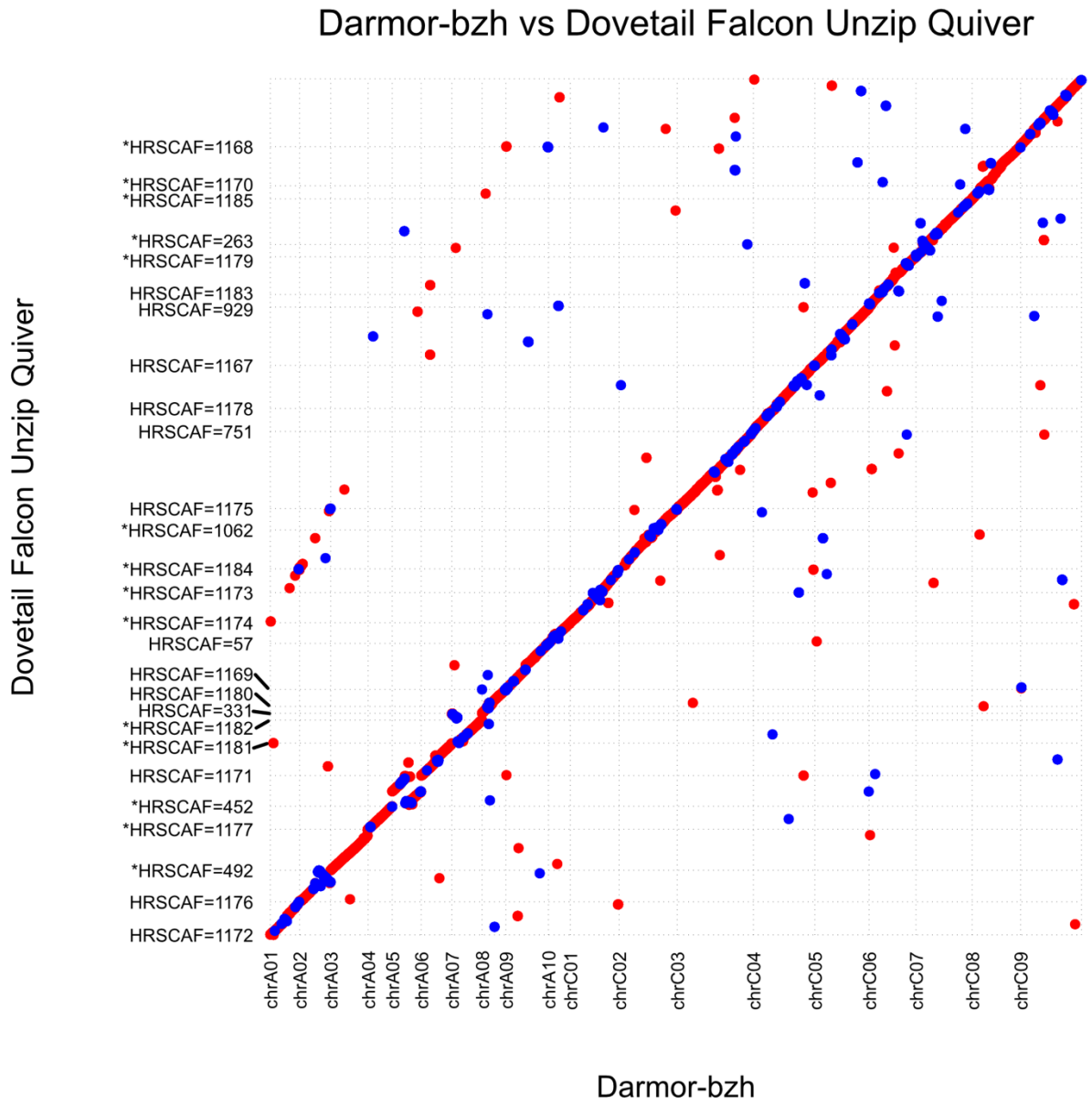

Figure 3 Nucmer plot of Dovetail_Falcon_Unzip_Quiver aligned to Brassica napus reference chromosomes. All sequences aligned are 1 Mbp or greater. A total of 27 Dovetail_Pilon_Canu scaffolds are aligned to 19 reference chromosomes. Red indicates an alignment in the forward direction and blue indicates an alignment in the reverse direction.

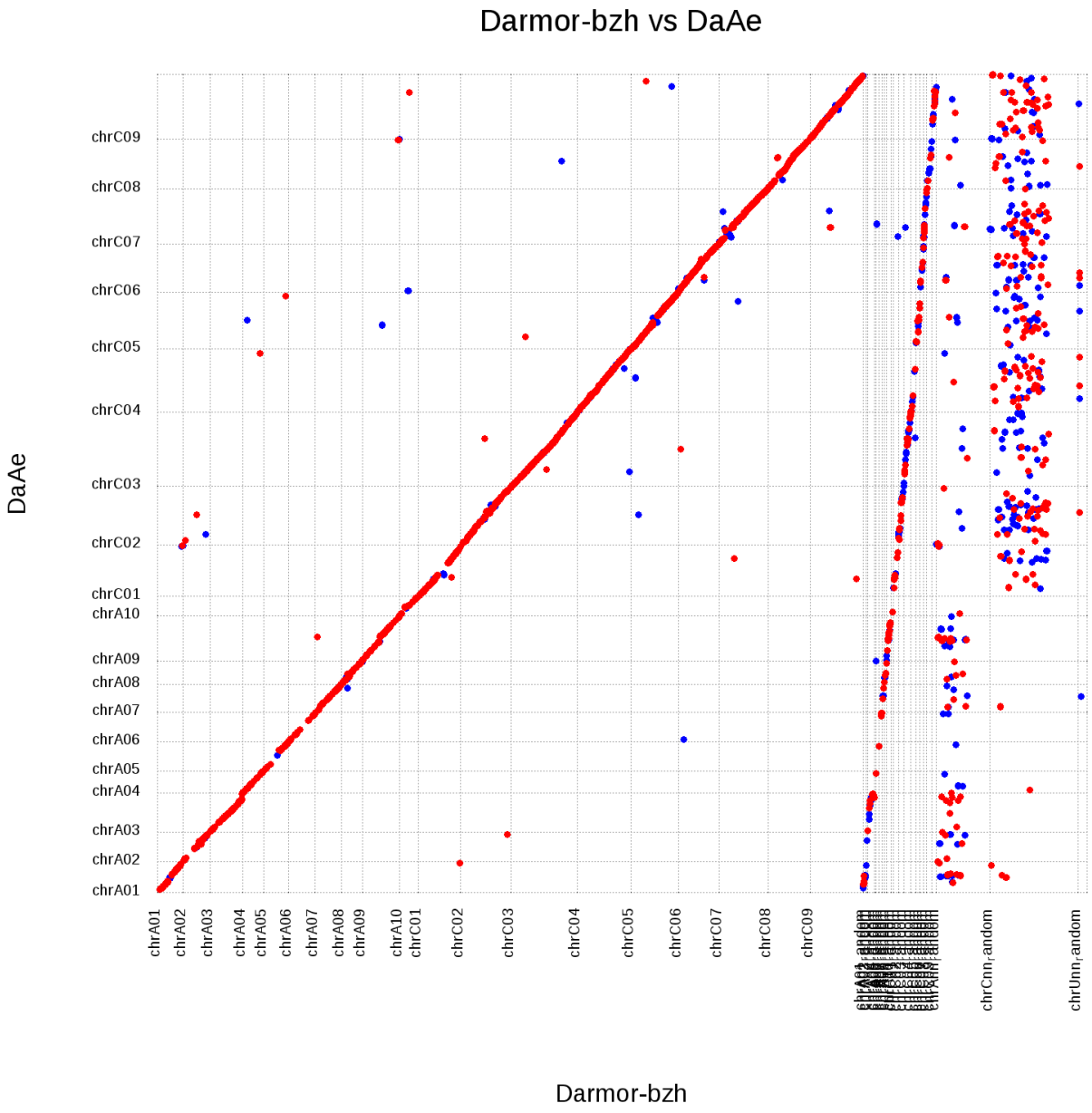

Figure 4 Nucmer plot of the final assembly aligned to the complete *Brassica napus* reference. A total of 19 final assembly pseudomolecules are aligned to 41 reference pseudomolecules. Reference pseudomolecules 1–19 are anchored and orientated sequences, reference pseudomolecules 20–38 contain sequences that could be anchored to a chromosome but could not be confidently positioned, reference pseudomolecules 39 and 40 contain sequences that could only be anchored to a subgenomes, and reference pseudomolecule 41 contains sequences that could not be anchored. Alignments of the final assembly to pseudomolecules 20–41 indicate regions where previously unanchored sequences were able to be placed in the new assembly. Red indicates an alignment in the forward direction and blue indicates an alignment in the reverse direction.

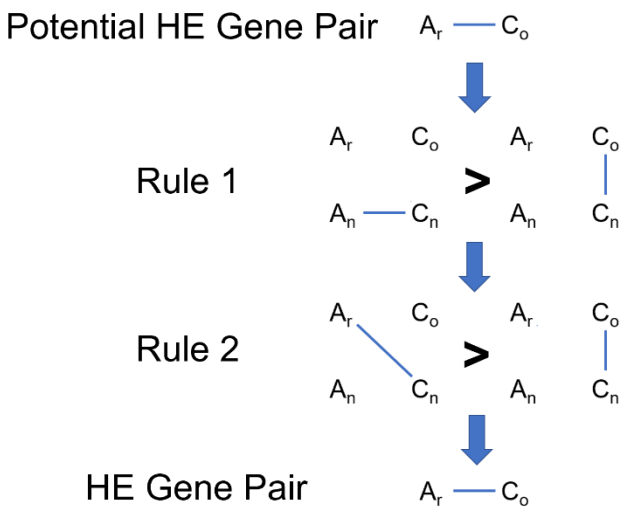

Figure 5 Example of a C gene being converted to an A gene. *B. rapa* = A_r, *B. oleracea* C_o, *B. napus* A = A_n, and *B. napus* C = C_n. A potential homoeologous gene pair must pass two rules. First, the C_n gene of the pair must align better to its homoeolog (A_n) than it does to its ortholog (C_o). Second, the C_n gene must also align better to its homoeolog's ortholog (A_r) than it does to its own ortholog (C_o). If both rules are satisfied, the pair is declared a homoeologous gene pair.

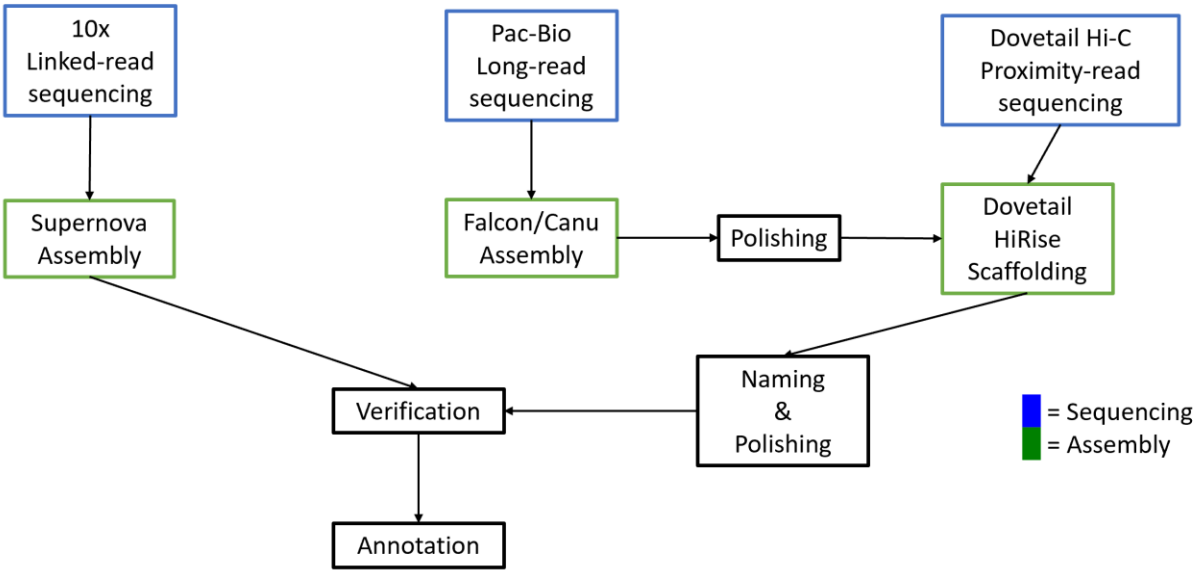

Figure 6 Genome assembly and annotation strategy.

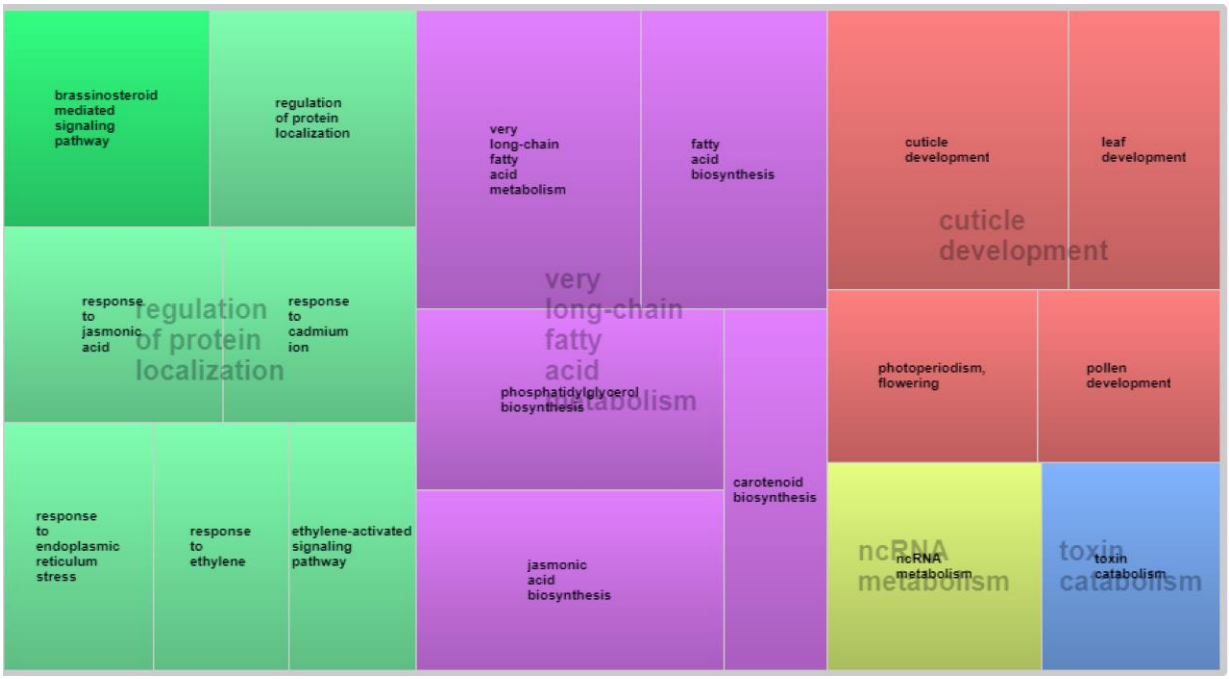

Figure 7 Revigo plot of over-represented GO terms of Brassica Unigene sequences present in the Da-Ae genome but not the Darmor-bzh genome.

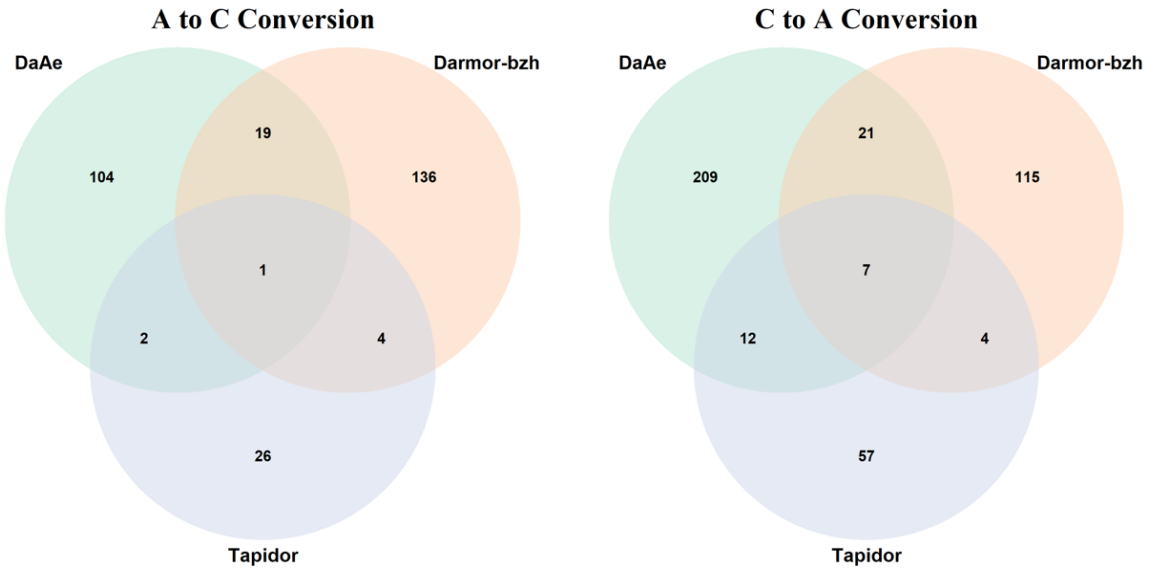

Figure 8 Conserved orthologous gene pairs between Da-Ae, the reference (Darmor-bzh), and Tapidor.

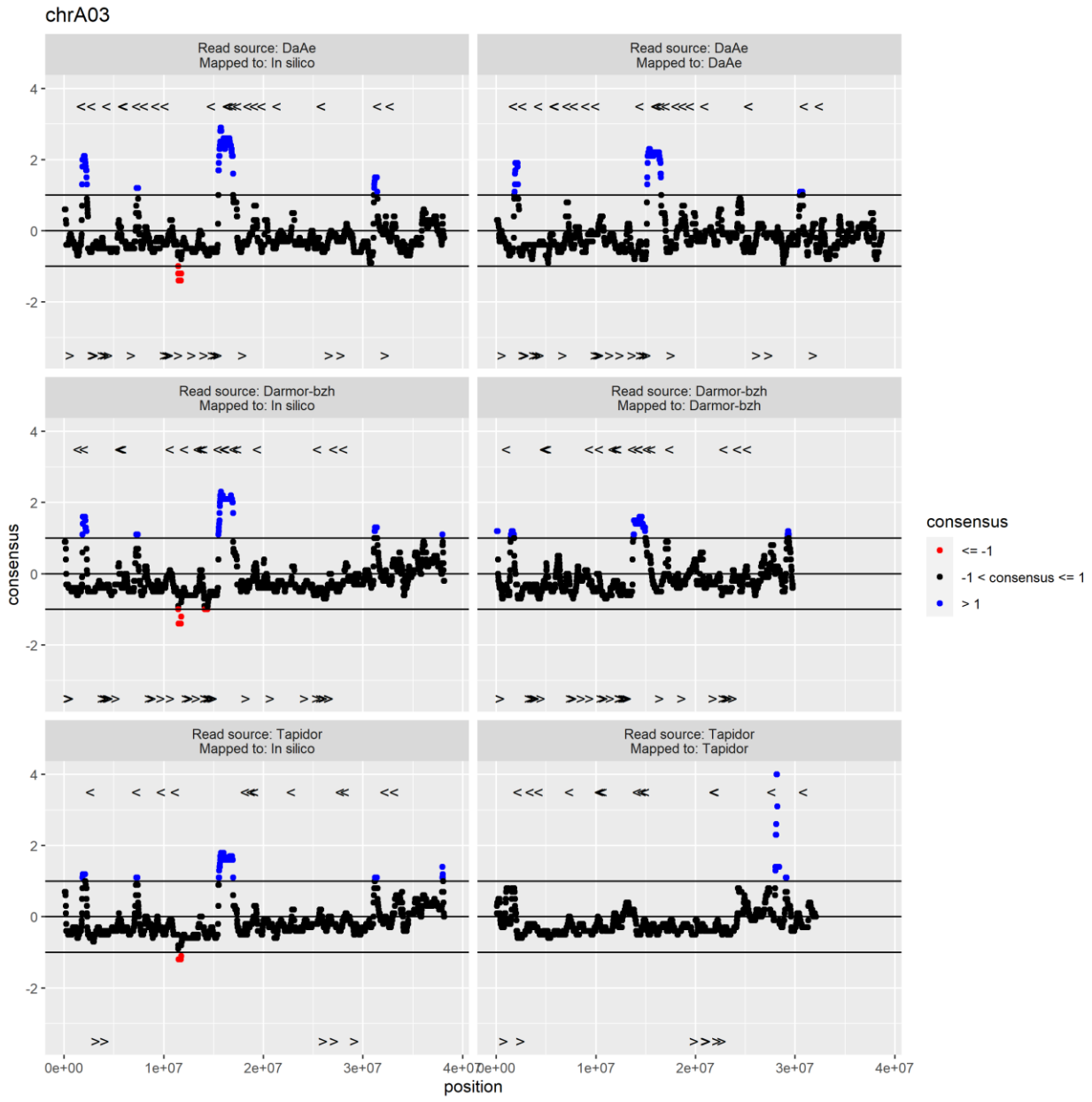

Figure 9 Coverage of each genome. There are three peaks of increased coverage shared among Da-Ae, Reference, and Tapidor, suggesting sites of shared homoeologous exchange. “<” indicates recipient and “>” indicates donor locations of genes suspected to be involved in homoeologous exchange.

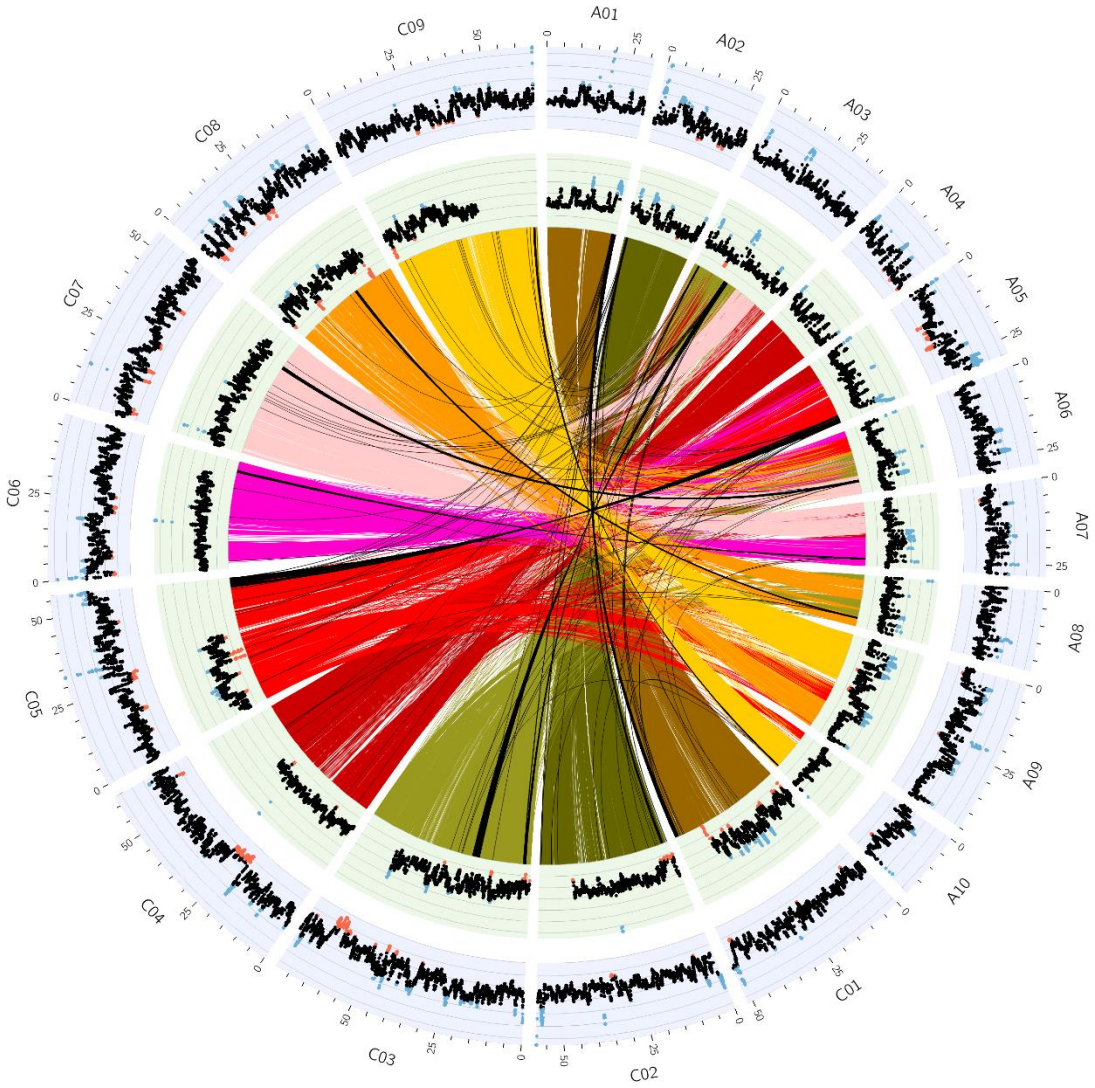

Figure 10 Circos plot of Da-Ae. Outer blue track is read coverage across the Da-Ae genome. Inner green track is read coverage across the *in silico* genome (*B. rapa* + *B. oleracea*). Blue dots indicate standardized coverage greater than 1 and red dots indicate standardized coverage less than -1. Ribbons in the center of the plot indicate regions of homology between the A and C subgenomes. Colors have been assigned based on C subgenome chromosomes. Black ribbons are regions suspected of having undergone homoeologous exchange.

Tables

Table 1 N50, number of sequences, total length, and percentages of BUSCOs. BUSCO percentages were calculated using the embryophyte odb9 dataset which contains 1,440 BUSCOS.

Assembly	N50 (Mbp)	Sequences	Total Length (Mbp)	Total Unambiguous Length (Mbp)	Gene Models	Complete BUSCOs	Complete single-copy BUSCOs	Complete duplicated BUSCOs	Fragmented BUSCOs	Missing BUSCOs
Darmor-bzh (Reference)	38.83	41	850.29	738.35	101,040	97.64	13.26	84.38	0.76	1.6
Da-Ae - Final	48.21	3,164	1,001.50	1,001.41	96,442	98.2	12.6	85.6	0.7	1.1
Darmor-bzh (19 pseudo molecules)	38.83	19	645.4	553.41	80,927	94.7	26.6	68.1	0.6	4.7
Da-Ae - Final (19 pseudo molecules)	51.43	19	816.17	816.08	88,605	98.1	12.1	86.0	0.6	1.3
Da-Ae Davis Supernova-1.1.5	0.14	80,371	793.05	677.83	NA	94.38	35	59.38	2.71	2.92
Da-Ae Novogene Supernova-1.1.5	0.14	81,812	805.97	693.95	NA	94.51	36.04	58.47	2.36	3.13
Da-Ae Davis Supernova-2	1.57	35,997	918.49	811.13	NA	97.57	19.44	78.13	0.83	1.60
B. rapa	2.03	16,823	334.23	319.72	NA	97.71	83.68	14.03	0.69	1.60
B. oleracea	2.52	19,955	571.25	534.67	NA	97.36	83.06	14.31	1.04	1.60
Da-Ae Falcon	1.79	1,852	889.44	889.44	NA	91.74	48.13	43.61	2.78	5.49
Da-Ae Falcon Unzip	1.80	1,541	878.51	878.51	NA	92.99	47.57	45.42	2.01	5.00
Da-Ae Falcon Unzip Quiver	1.80	1,508	880.99	880.99	NA	98.26	17.43	80.83	0.49	1.25
Da-Ae Pilon Falcon Unzip Quiver	1.80	1,508	880.87	880.87	NA	98.26	14.79	83.47	0.56	1.18
Da-Ae Dovetail Falcon Unzip Quiver	35.52	709	881.08	880.99	NA	98.26	17.99	80.28	0.55	1.19
Da-Ae Canu	1.59	4,008	1,004.00	1,004.00	NA	98.06	15.42	82.64	0.69	1.25
Da-Ae Pilon_Canu	1.59	4,008	1,003.52	1,003.52	NA	98.19	13.68	84.51	0.63	1.2
DA-Ae Dovetail_Pilon_Canu	42.79	3,190	1,003.60	1,003.52	NA	98.33	13.61	84.72	0.55	1.1

Table 2 Shared Single Copy BUSCOs

BUSCO ID	DaAe	Darmor-bzh	Tapidor	B. rapa	B. oleracea	Description
EOG093600DF	chrA06	chrA06	chrC07	chrA06	chrC07	XPG/Rad2 endonuclease
EOG093602FO	chrC02	chrC02	chrC02	chrA02	chrC02	Pentatricopeptide repeat
EOG093602X4	chrA07	chrA07	chrA07	chrA07	chrC06	Uncharacterized protein
EOG09360317	chrC04	chrA05	chrC04	chrA05	chrC04	Ribosomal protein S5 domain 2-type fold
EOG093603PK	chrA05	chrA05	chrA05	chrA05	chrC05	NHL domain-containing protein
EOG093604B8	chrA07	chrA07	chrA07	chrA07	chrC06	Golgi transport complex protein-related
EOG093604D4	chrC02	chrC02	chrC02	chrA02	chrC02	Elongation factor G, III-V domain
EOG0936055R	chrA01	chrA01	chrA02	chrA01	chrC01	WW domain-containing protein
EOG093605DD	chrC09	chrA10	chrC09	chrA10	chrC09	Protein kinase domain
EOG093605ZP	chrC08	chrC08	chrA01	chrA08	chrC08	Cytochrome P450
EOG093608BO	chrC08	chrC08	chrC08	chrA09	chrC08	Putative uncharacterized protein
EOG09360B5S	chrA06	chrA06	chrA06	chrA06	chrC07	Peptidase C78, ubiquitin fold modifier-specific peptidase 1/ 2
EOG09360CRR	chrC03	chrA02	chrA02	chrA02	chrC03	Uncharacterized protein
EOG09360DWT	chrC06	chrC06	chrC02	chrA05	chrC03	Peptide chain release factor
EOG09360ETX	chrA06	chrA06	chrA02	chrA06	chrC07	Histone deacetylase superfamily
EOG09360EX7	chrA02	chrC02	chrA02	chrA02	chrC02	HAUS augmin-like complex subunit 7-like
EOG09360FOF	chrA02	chrC02	chrC02	chrA02	chrC02	SRP40, C-terminal
EOG09360G99	chrA02	chrA02	chrA02	chrA02	chrC02	Uncharacterized protein
EOG09360IS4	chrC07	chrC07	chrC04	chrA07	chrC09	Serine-threonine protein kinase 19

EOG09360MCO	chrA05	chrC04	chrA07	chrA05	chrC04	ubiquitin family protein
EOG09360N2Y	chrA09	chrA09	chrC09	chrA09	chrC09	Oxoglutarate/iron-dependent dioxygenase
EOG09360PV7	chrA10	chrC05	chrA10	chrA10	chrC05	Prefoldin
EOG09360QHJ	chrC03	chrC03	chrC03	chrA03	chrC03	heat shock protein DnaJ, putative, expressed
EOG09360ZSS	chrA07	chrA07	chrC06	chrA07	chrC06	Uncharacterized protein

Table 3 Comparison of assembly statistics. Percentages indicate percent change of Da-Ae assembly relative to Darmor-bzh.

	N50	Unambiguous Bases	Gene Models	Complete BUSCOs
Full Assembly	124%	136%	95%	101%
Pseudo Molecules	132%	147%	109%	104%

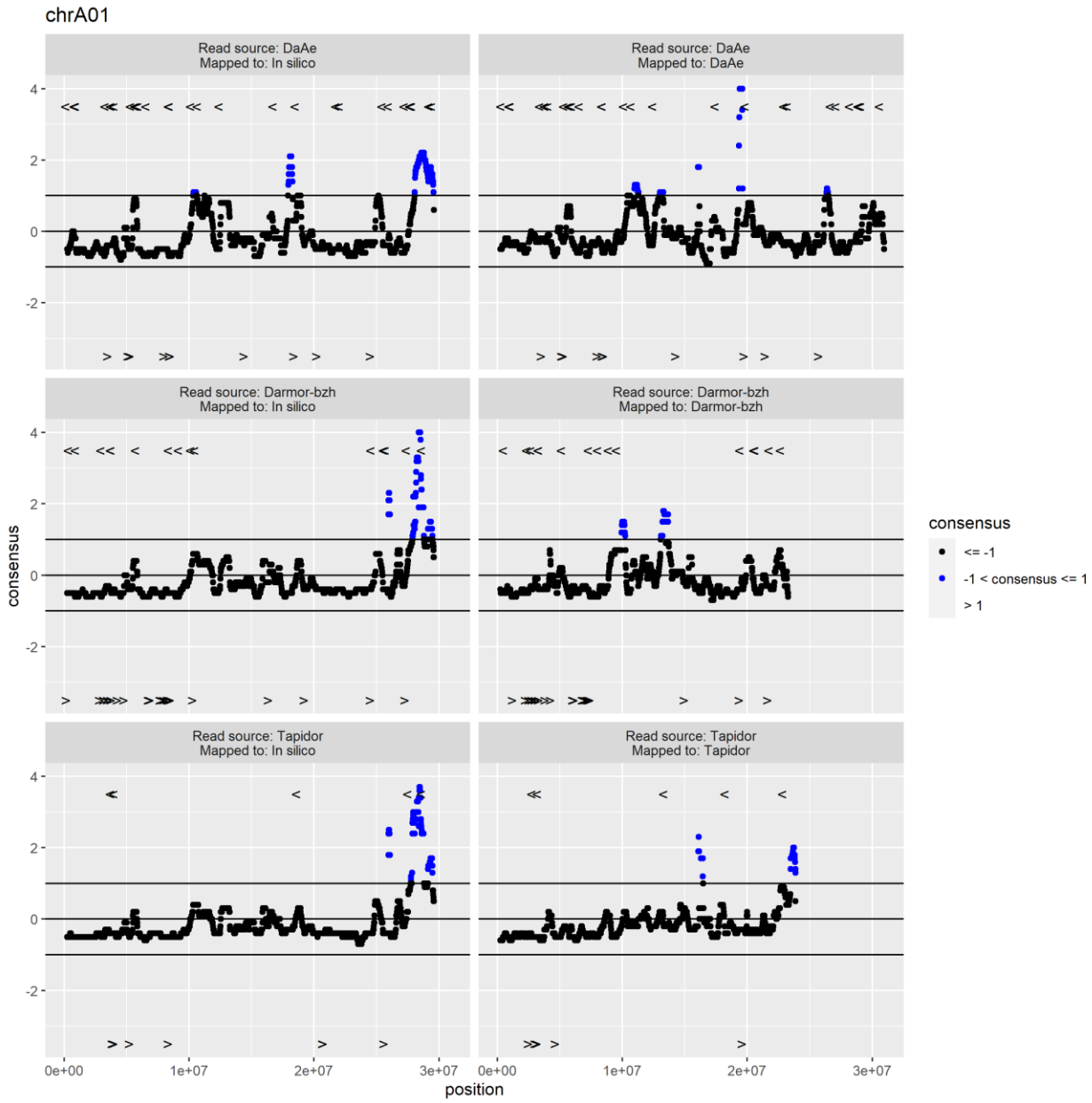

Supplementary Figure 1 Coverage of each genome. "<" indicates recipient and ">" indicates donor locations of genes suspected to be involved in homoeologous exchange.

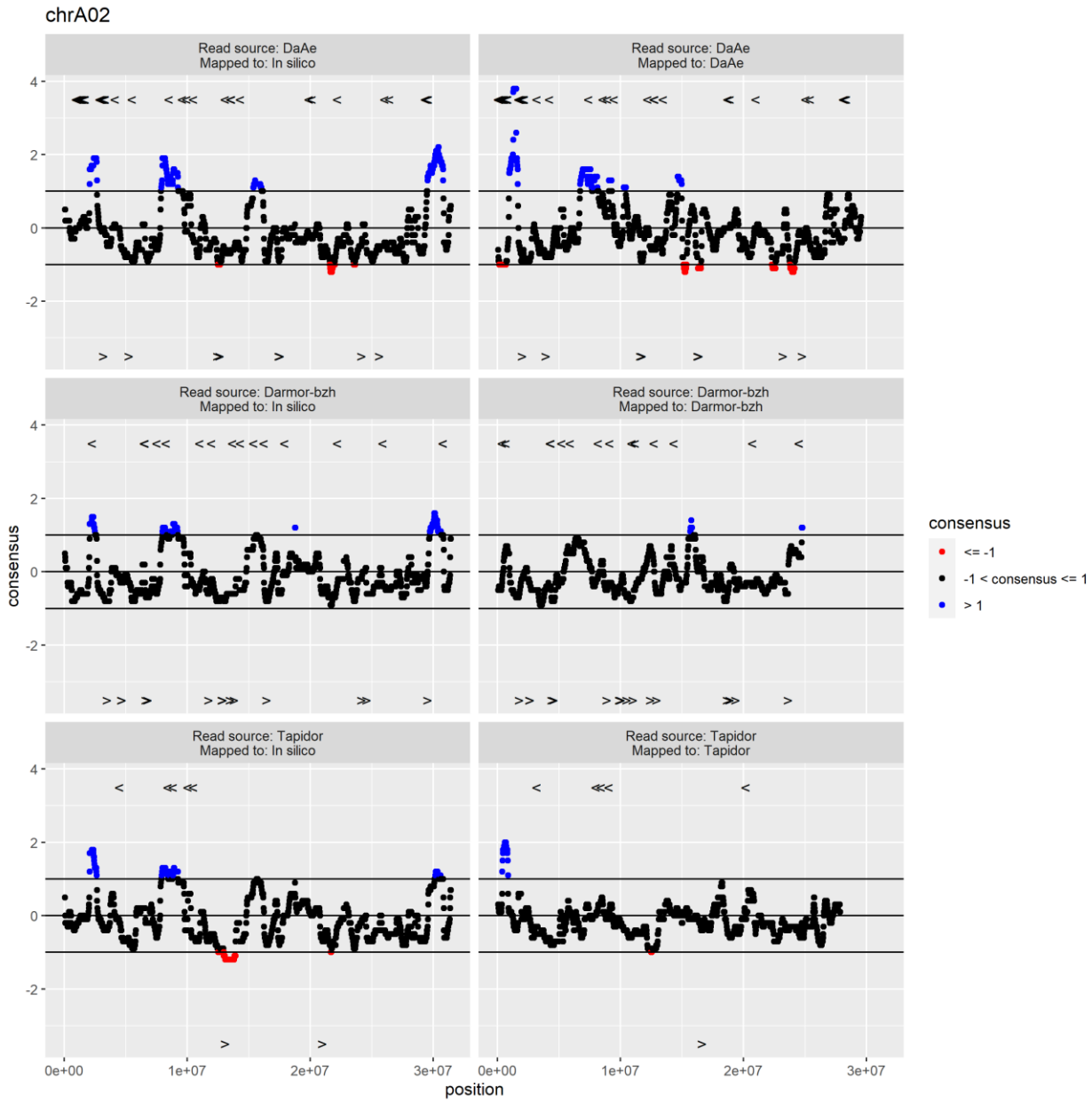

Supplementary Figure 2 Coverage of each genome. "<" indicates recipient and ">" indicates donor locations of genes suspected to be involved in homoeologous exchange.

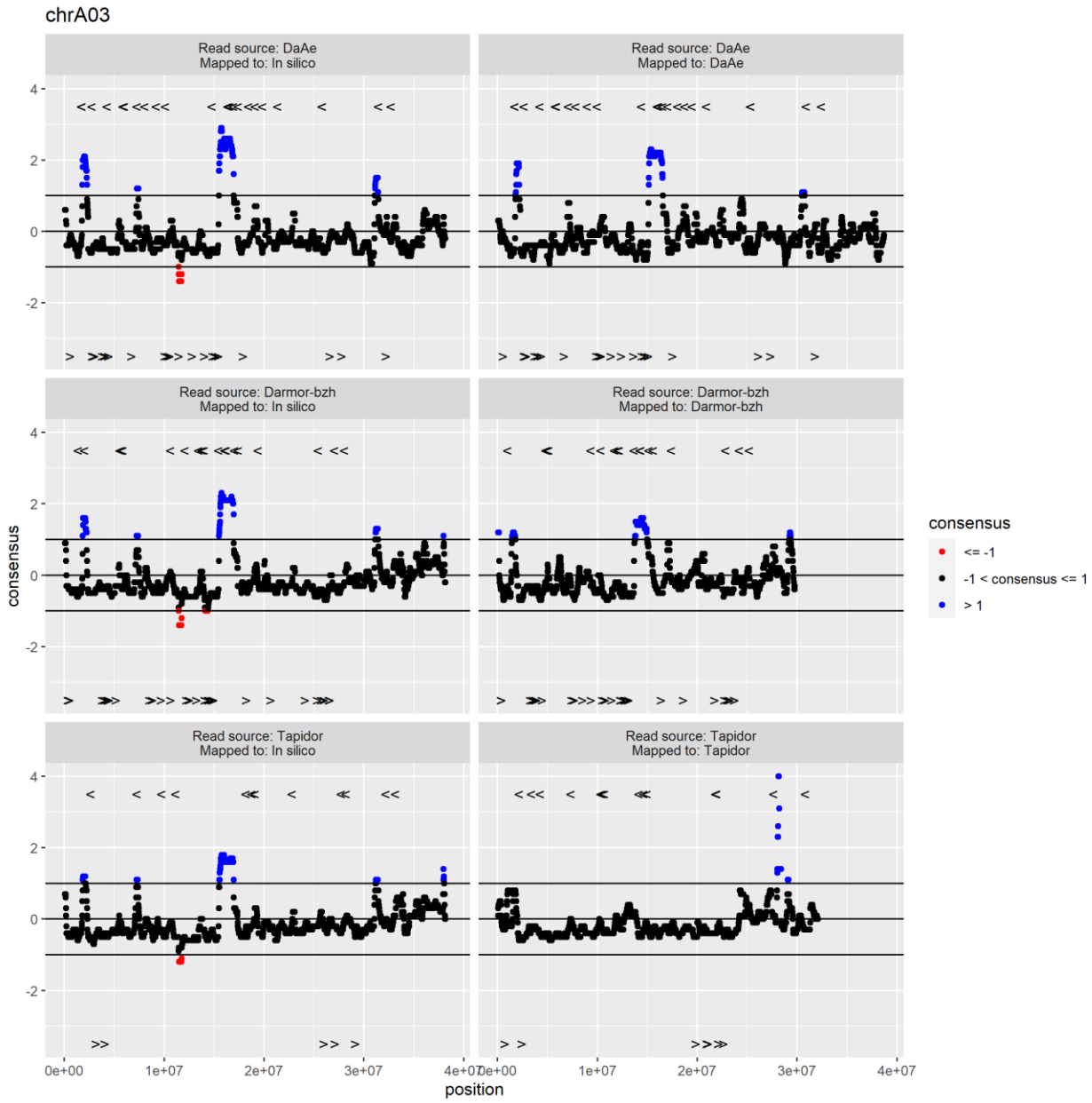

Supplementary Figure 3 Coverage of each genome. "<" indicates recipient and ">" indicates donor locations of genes suspected to be involved in homoeologous exchange.

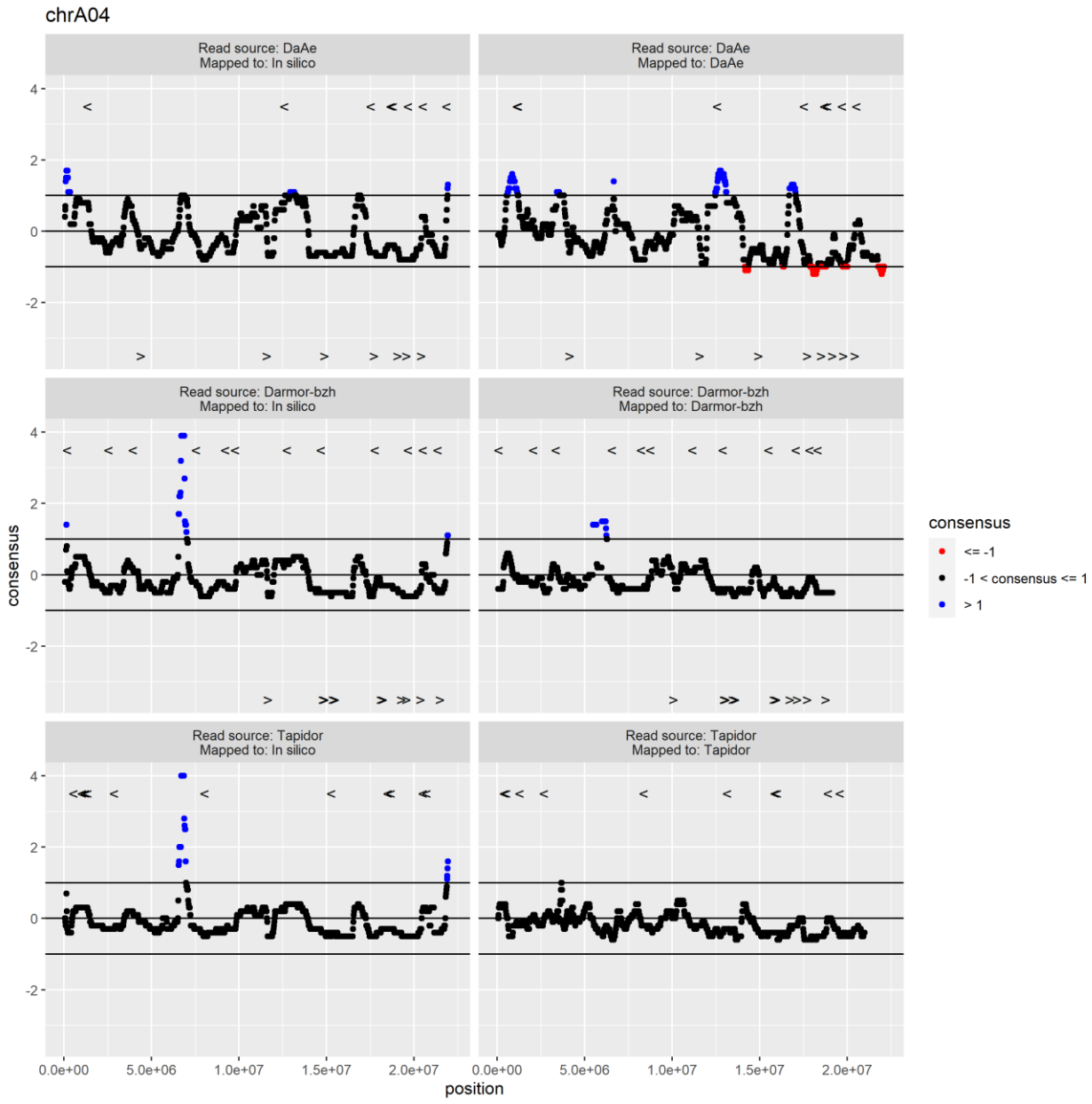

Supplementary Figure 4 Coverage of each genome. "<" indicates recipient and ">" indicates donor locations of genes suspected to be involved in homoeologous exchange.

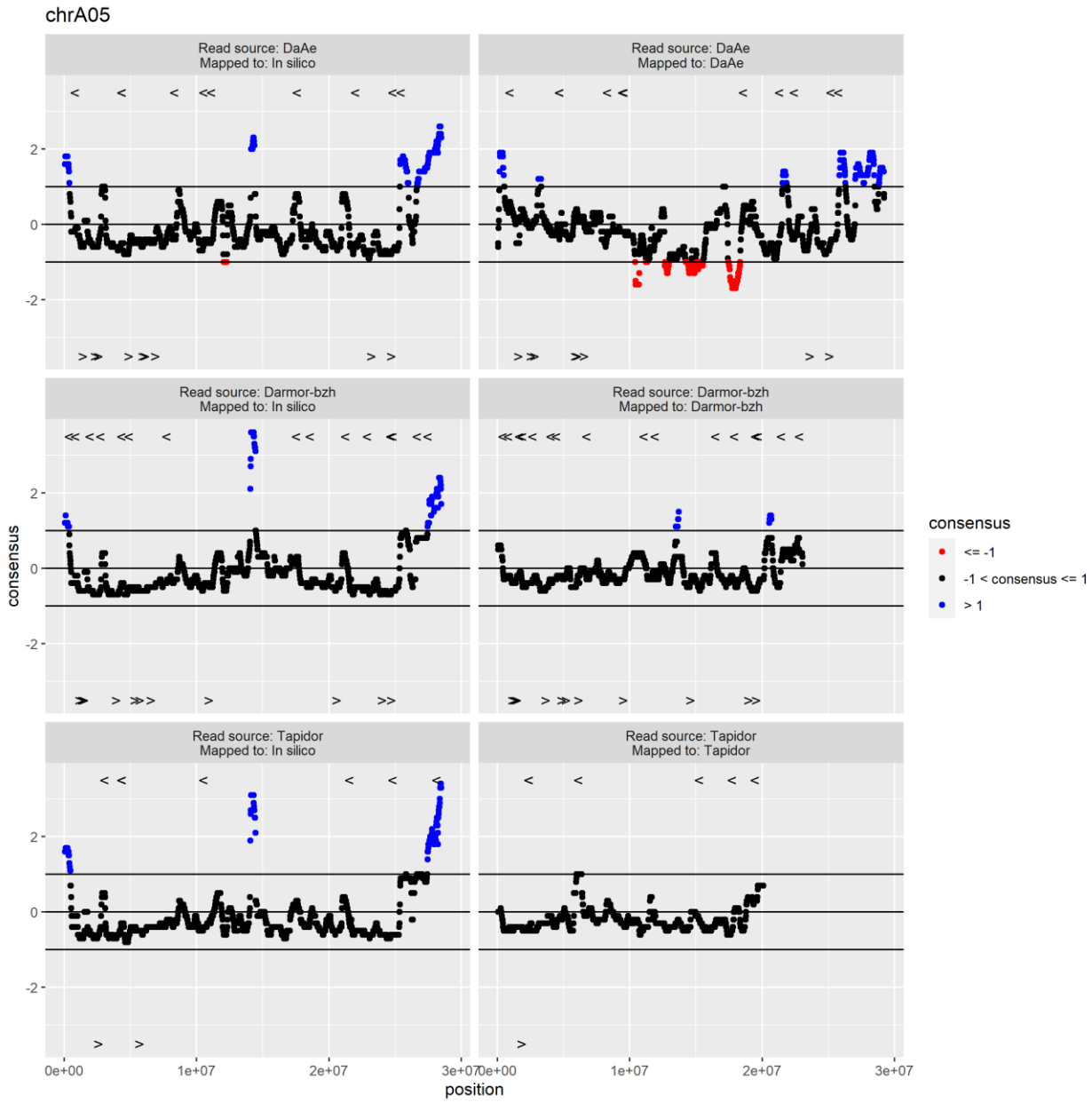

Supplementary Figure 5 Coverage of each genome. "<" indicates recipient and ">" indicates donor locations of genes suspected to be involved in homoeologous exchange.

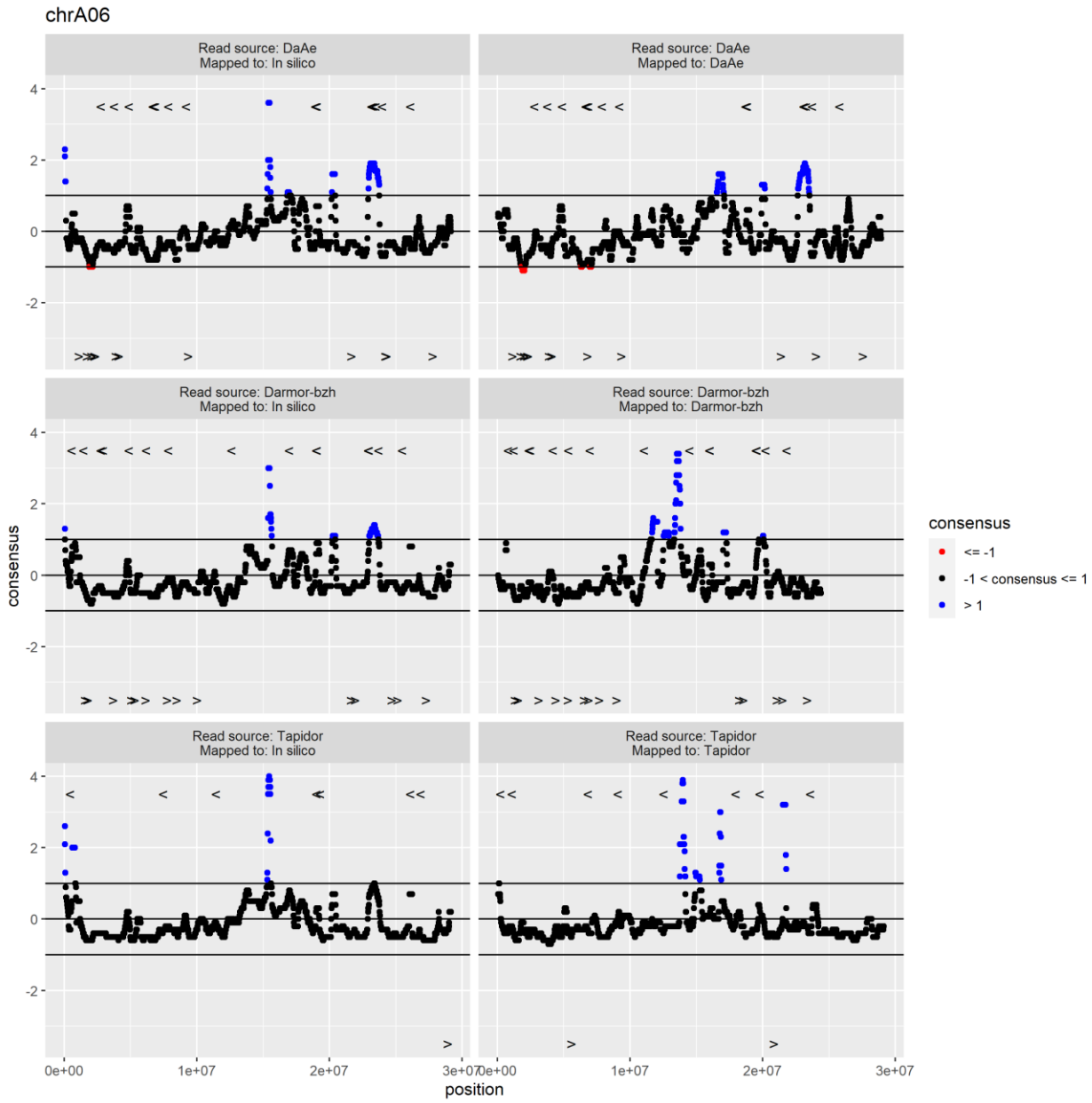

Supplementary Figure 6 Coverage of each genome. "<" indicates recipient and ">" indicates donor locations of genes suspected to be involved in homoeologous exchange.

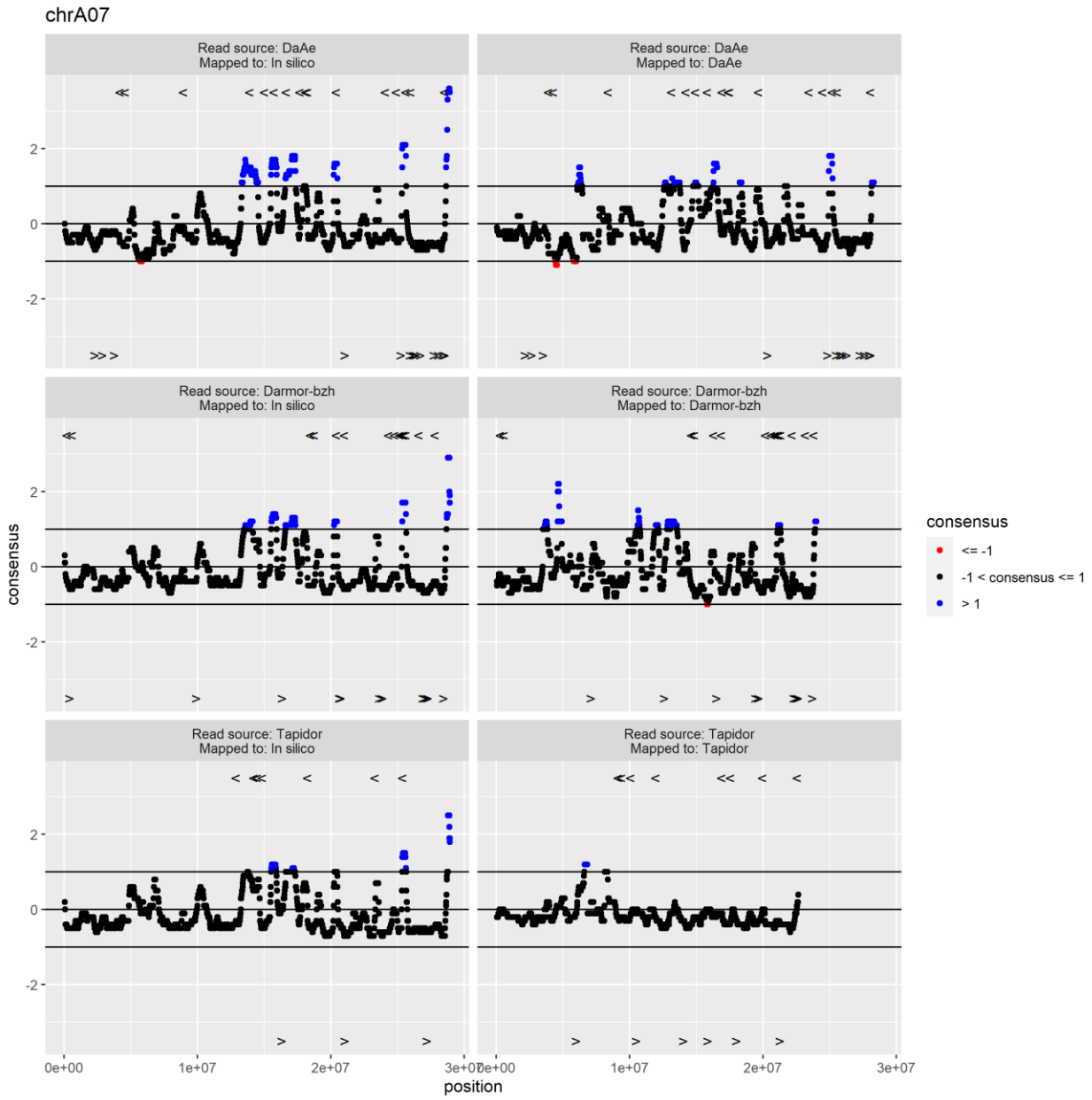

Supplementary Figure 7 Coverage of each genome. "<" indicates recipient and ">" indicates donor locations of genes suspected to be involved in homoeologous exchange.

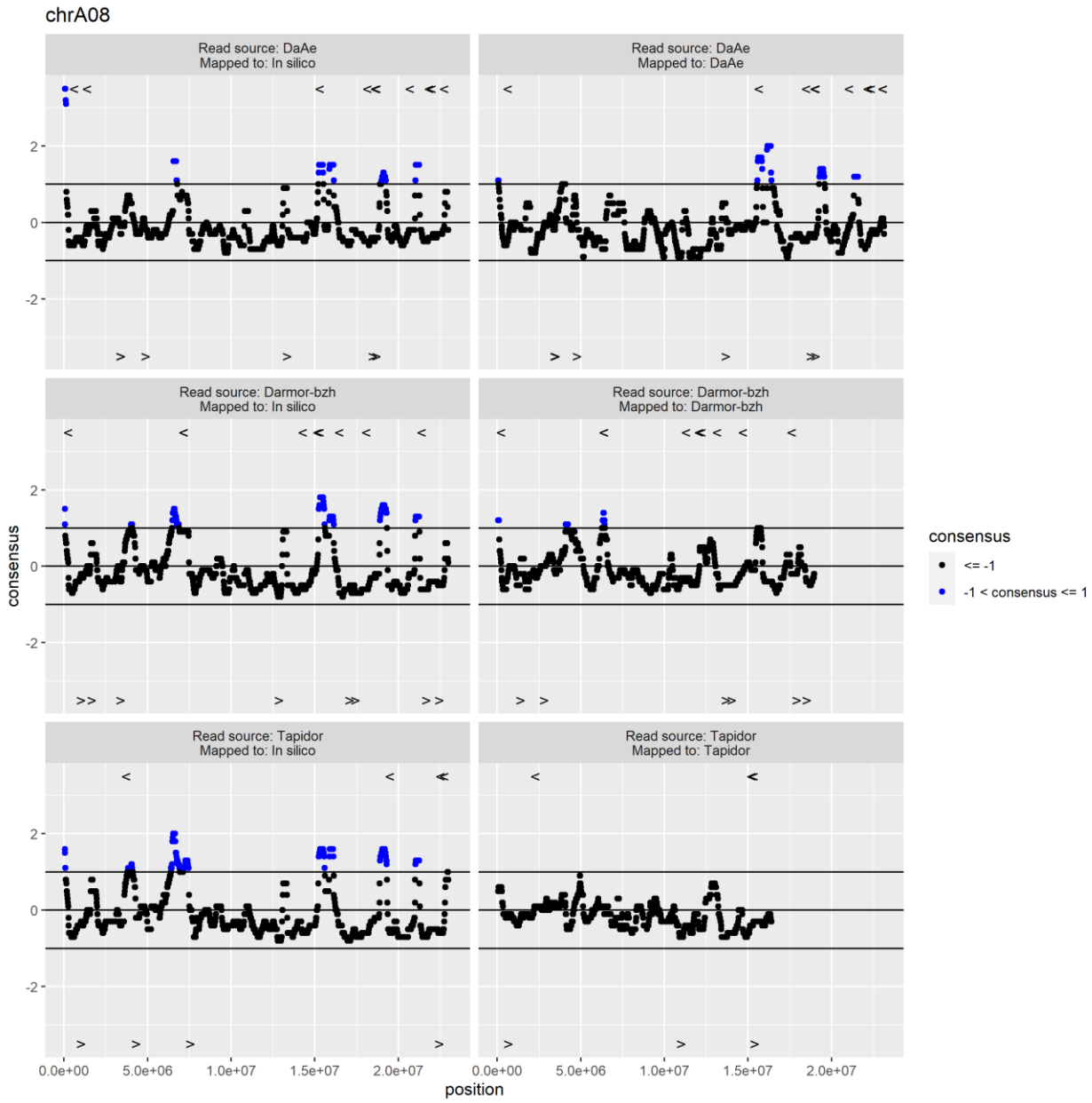

Supplementary Figure 8 Coverage of each genome. "<" indicates recipient and ">" indicates donor locations of genes suspected to be involved in homoeologous exchange.

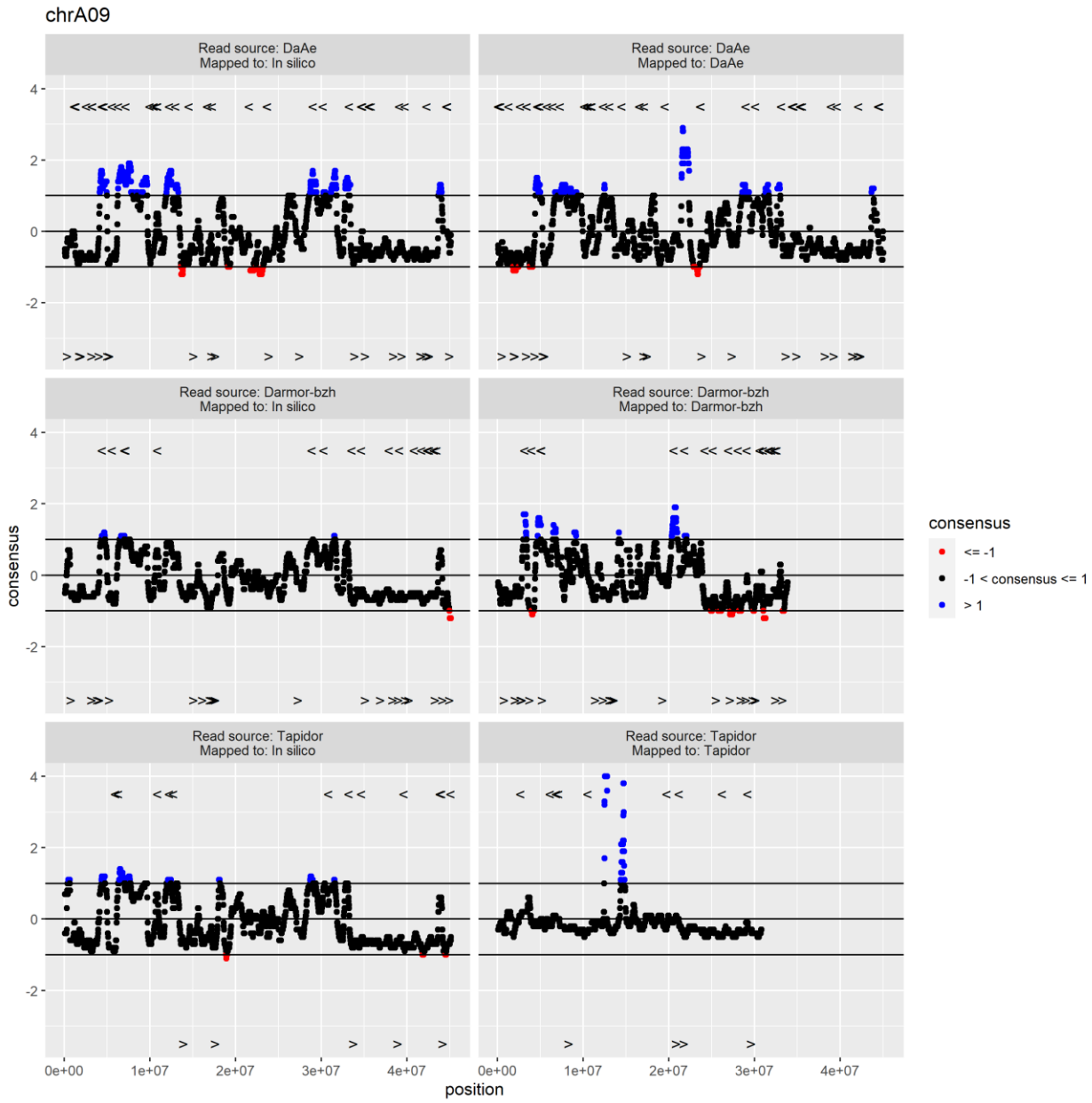

Supplementary Figure 9 Coverage of each genome. "<" indicates recipient and ">" indicates donor locations of genes suspected to be involved in homoeologous exchange.

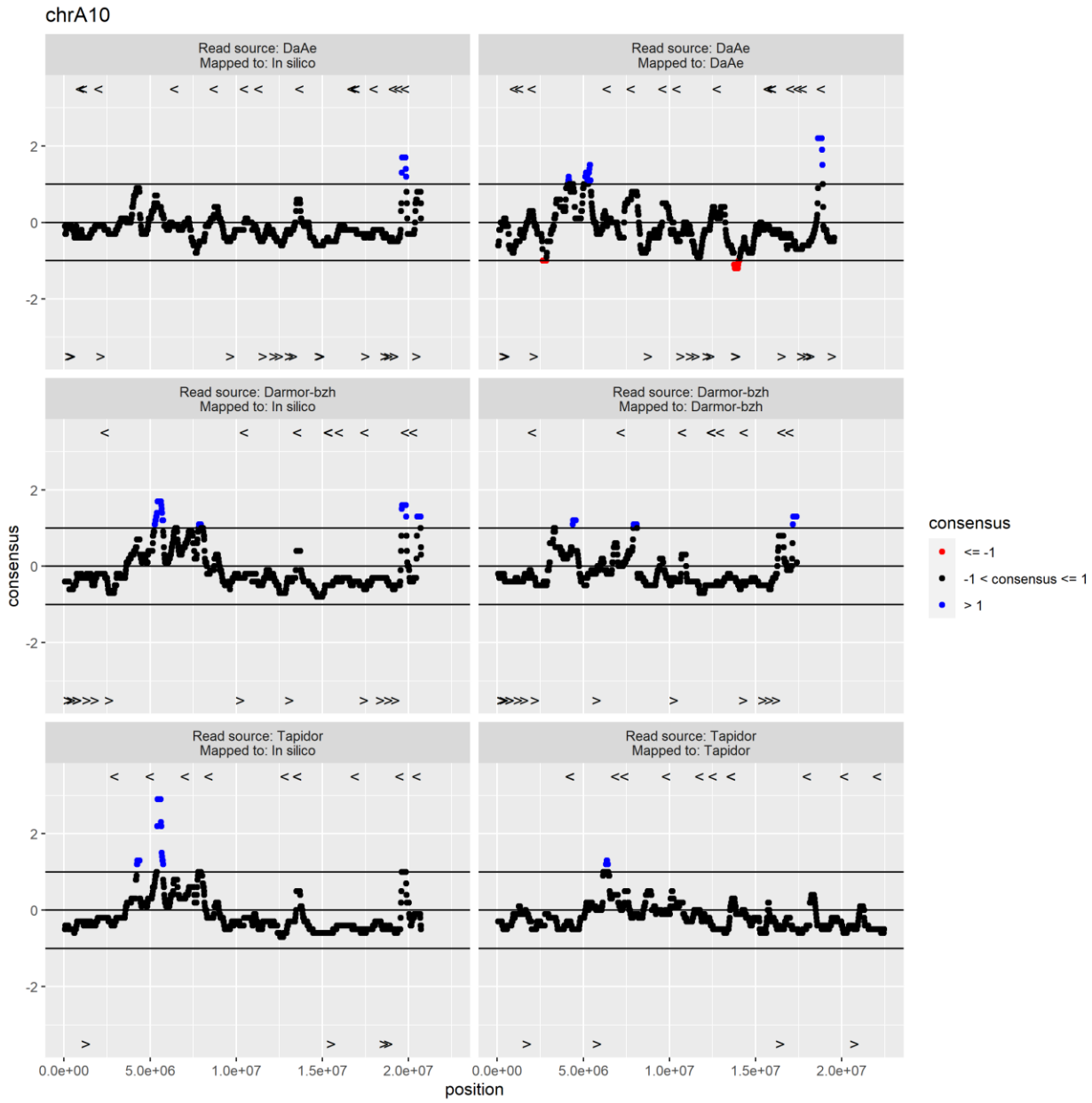

Supplementary Figure 10 Coverage of each genome. "<" indicates recipient and ">" indicates donor locations of genes suspected to be involved in homoeologous exchange.

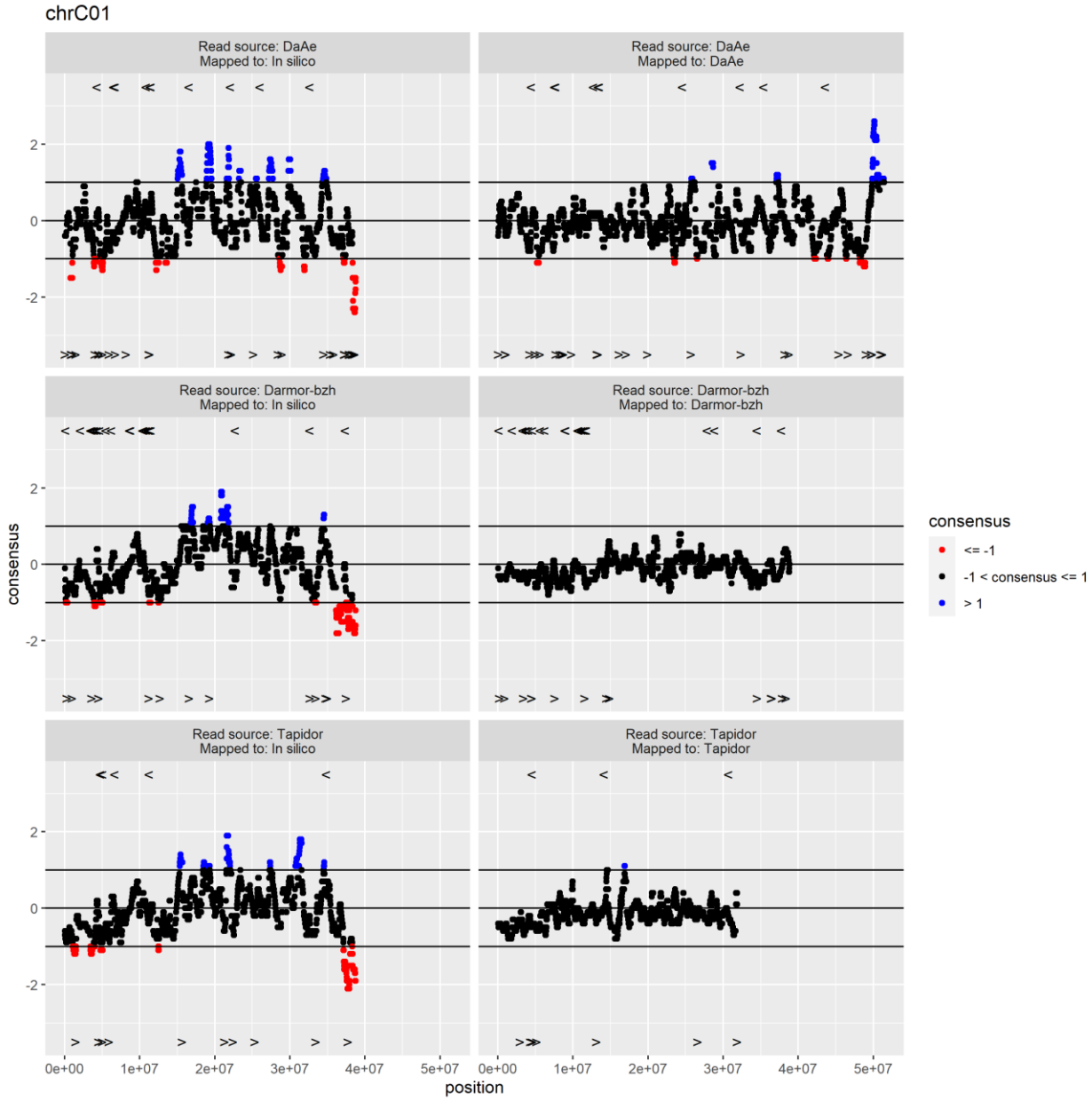

Supplementary Figure 11 Coverage of each genome. "<" indicates recipient and ">" indicates donor locations of genes suspected to be involved in homoeologous exchange.

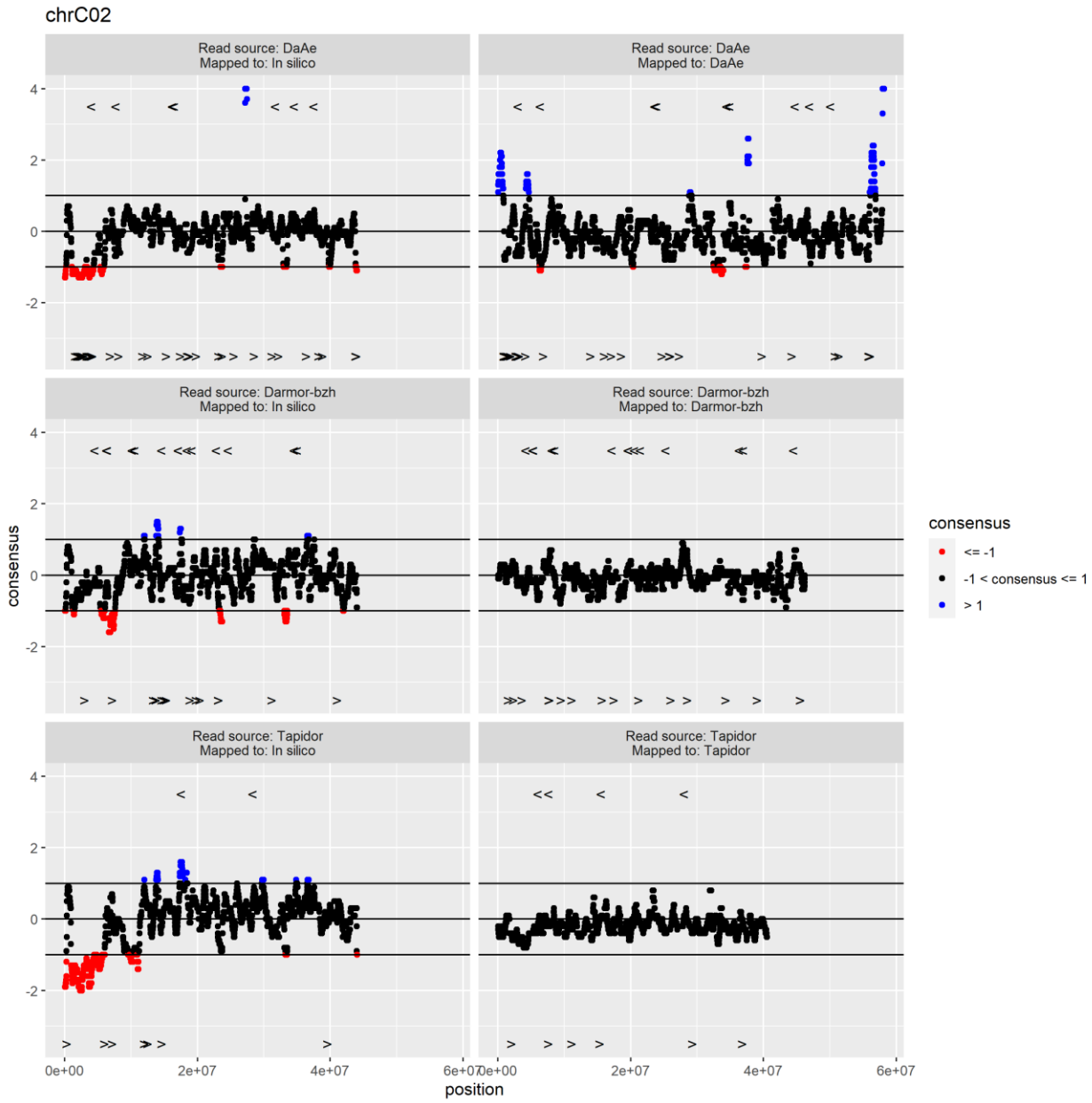

Supplementary Figure 12 Coverage of each genome. "<" indicates recipient and ">" indicates donor locations of genes suspected to be involved in homoeologous exchange.

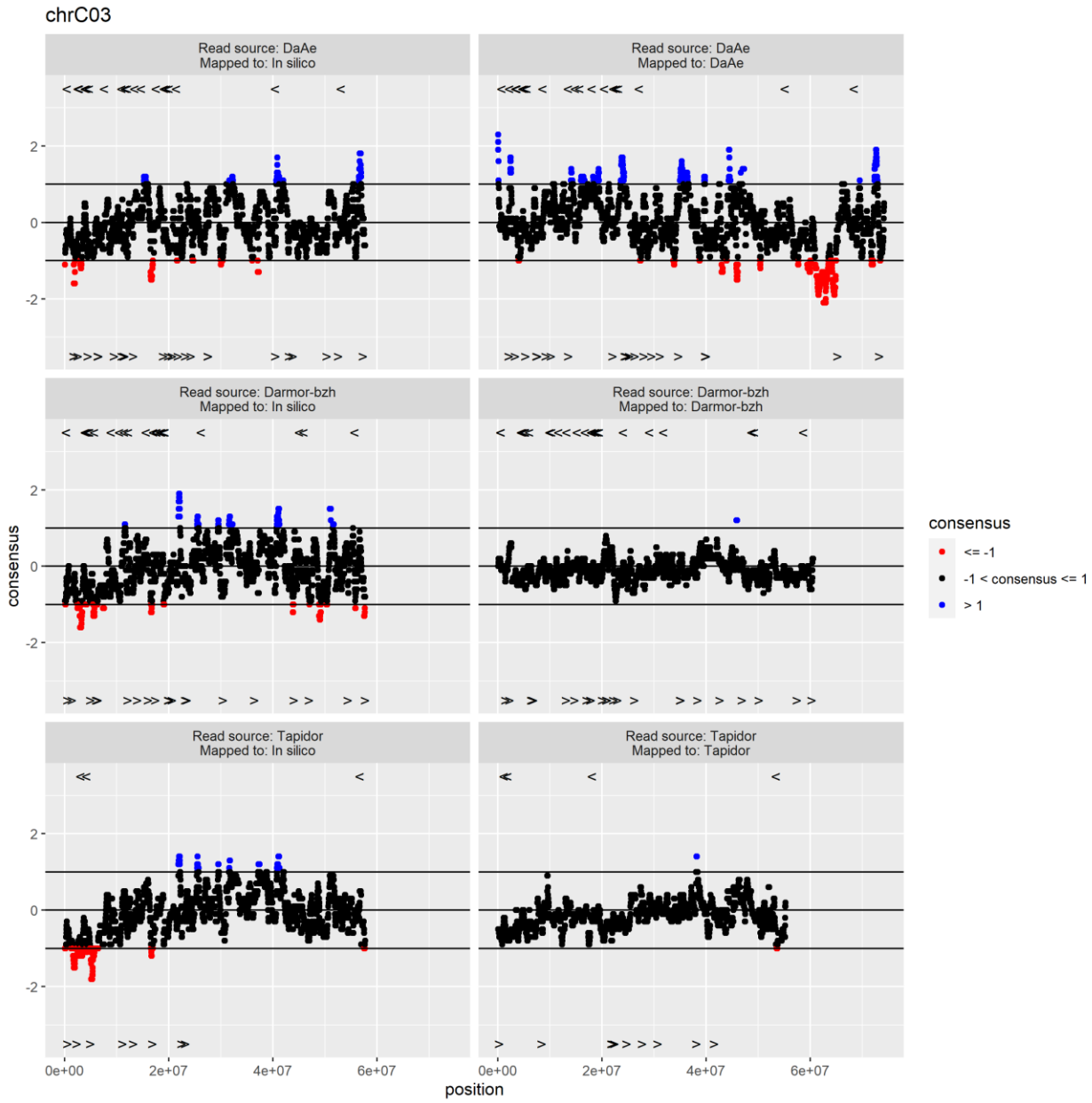

Supplementary Figure 13 Coverage of each genome. "<" indicates recipient and ">" indicates donor locations of genes suspected to be involved in homoeologous exchange.

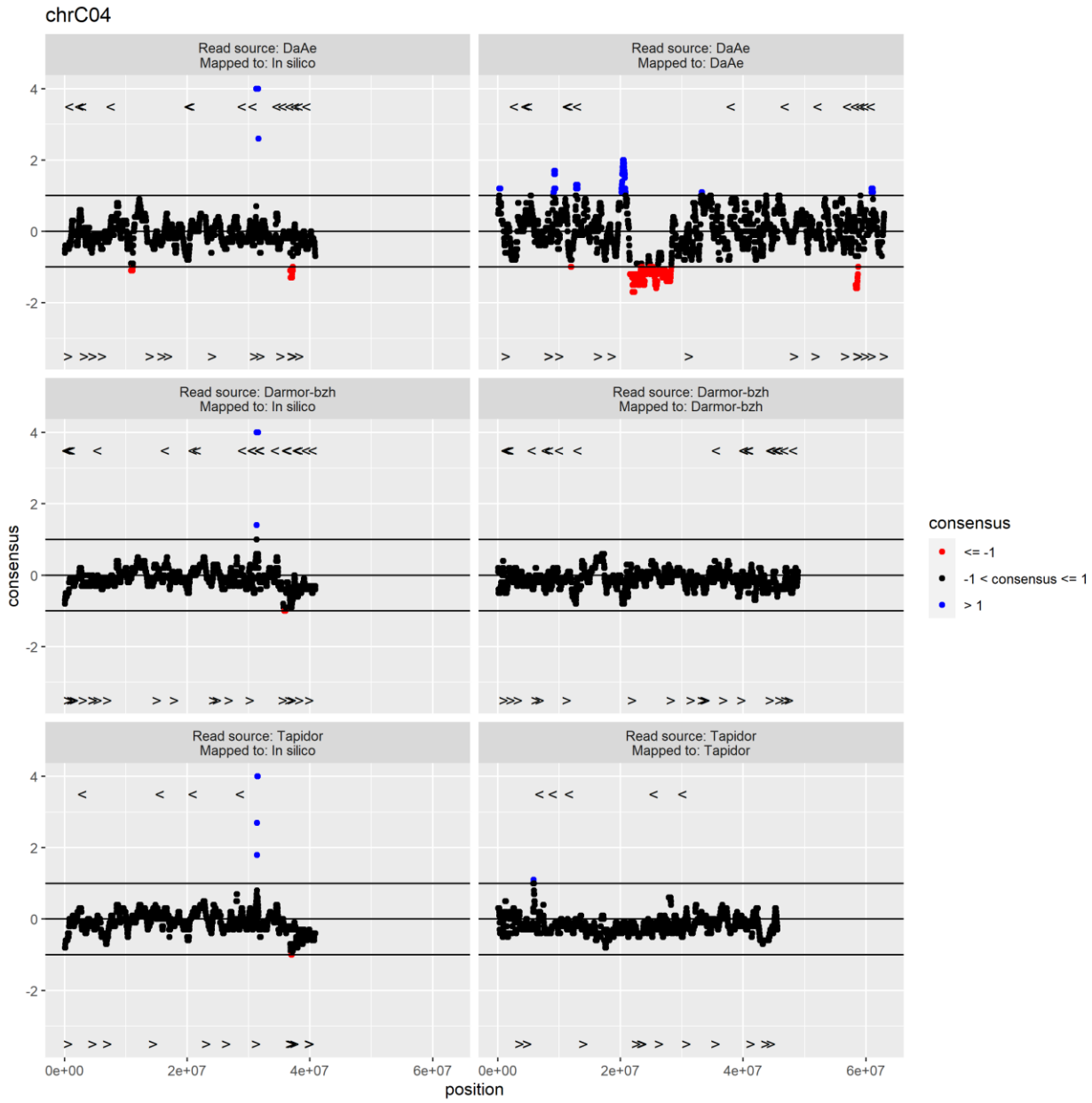

Supplementary Figure 14 Coverage of each genome. "<" indicates recipient and ">" indicates donor locations of genes suspected to be involved in homoeologous exchange.

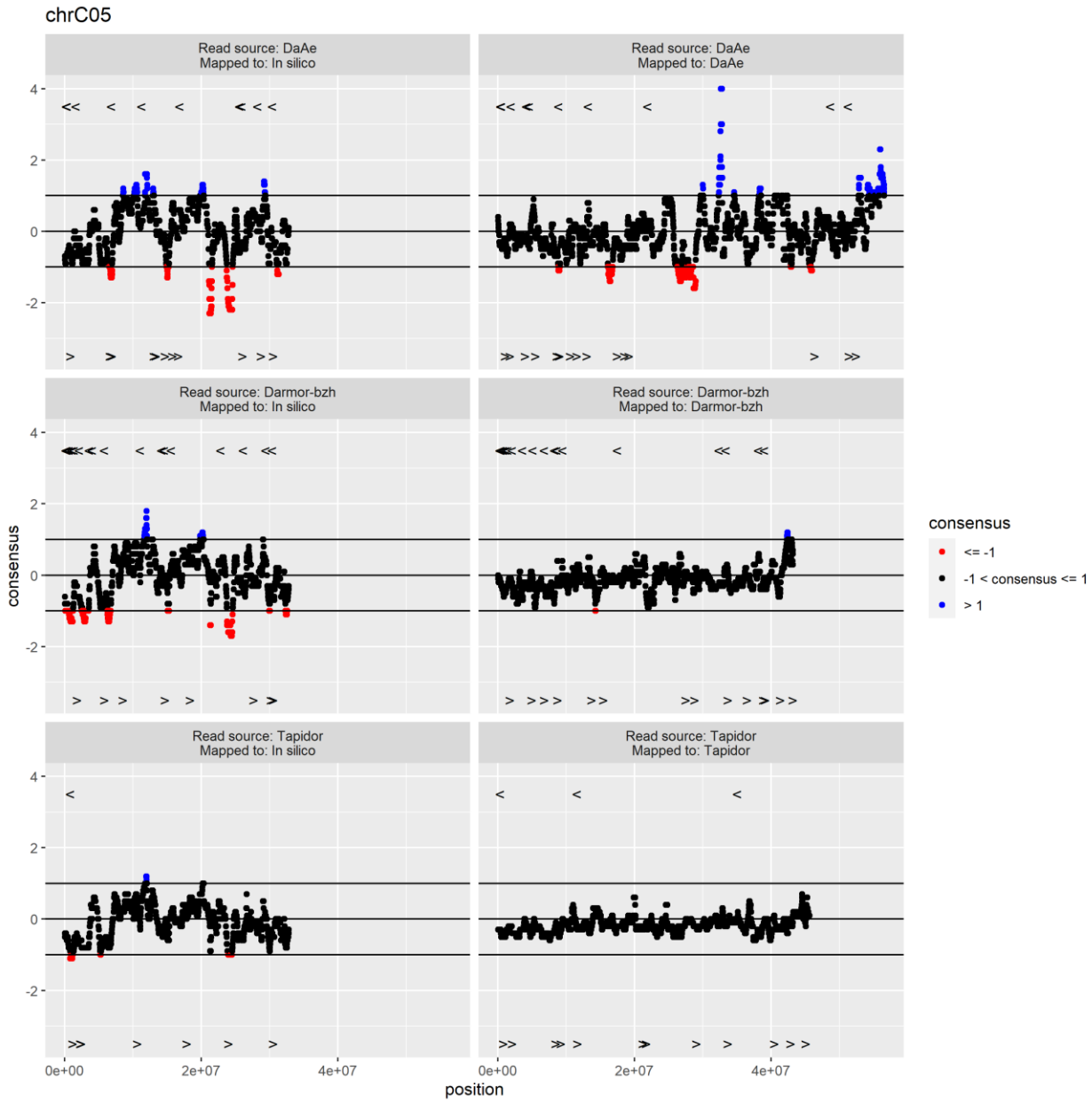

Supplementary Figure 15 Coverage of each genome. "<" indicates recipient and ">" indicates donor locations of genes suspected to be involved in homoeologous exchange.

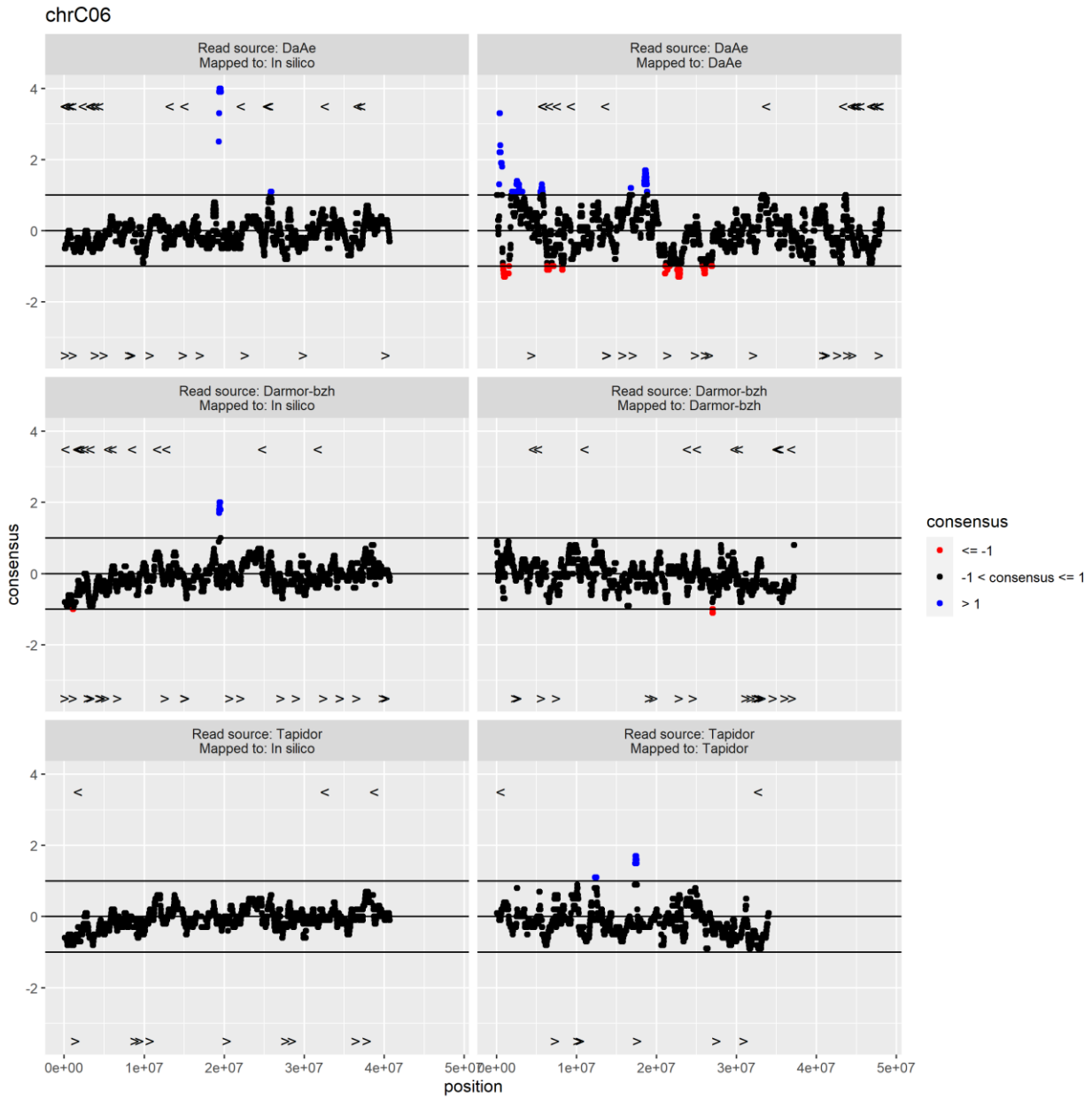

Supplementary Figure 16 Coverage of each genome. "<" indicates recipient and ">" indicates donor locations of genes suspected to be involved in homoeologous exchange.

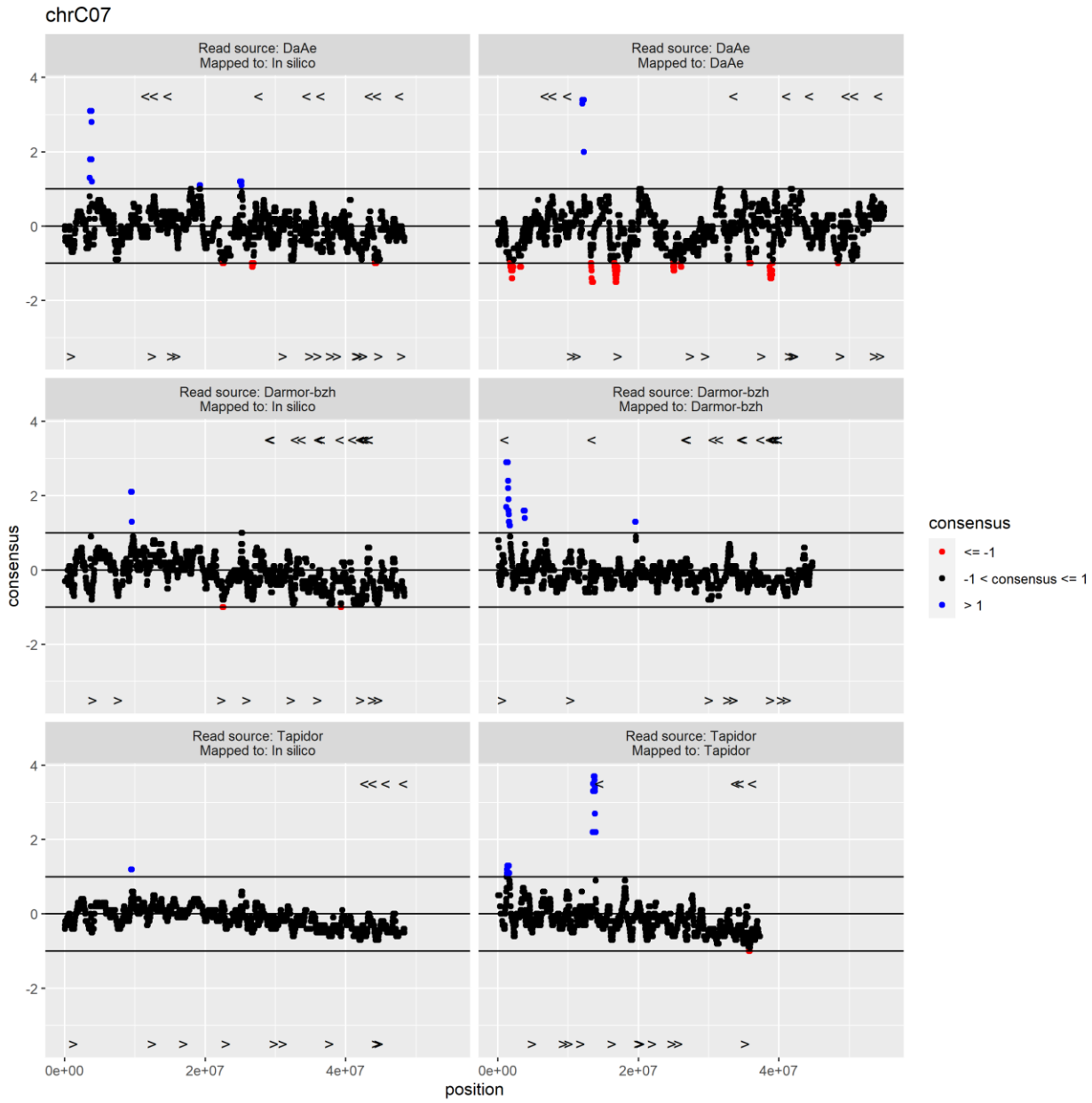

Supplementary Figure 17 Coverage of each genome. "<" indicates recipient and ">" indicates donor locations of genes suspected to be involved in homoeologous exchange.

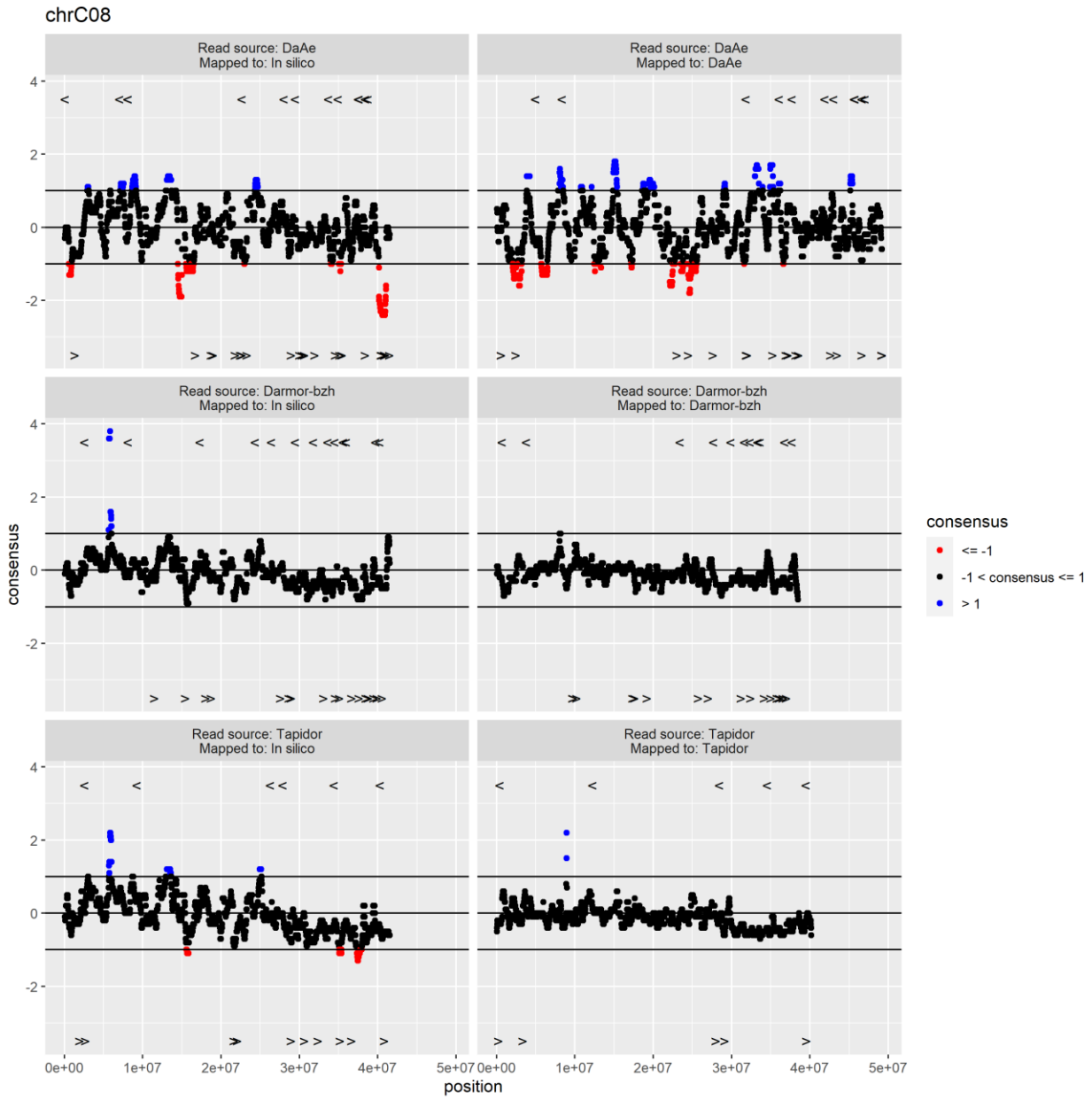

Supplementary Figure 18 Coverage of each genome. "<" indicates recipient and ">" indicates donor locations of genes suspected to be involved in homoeologous exchange.

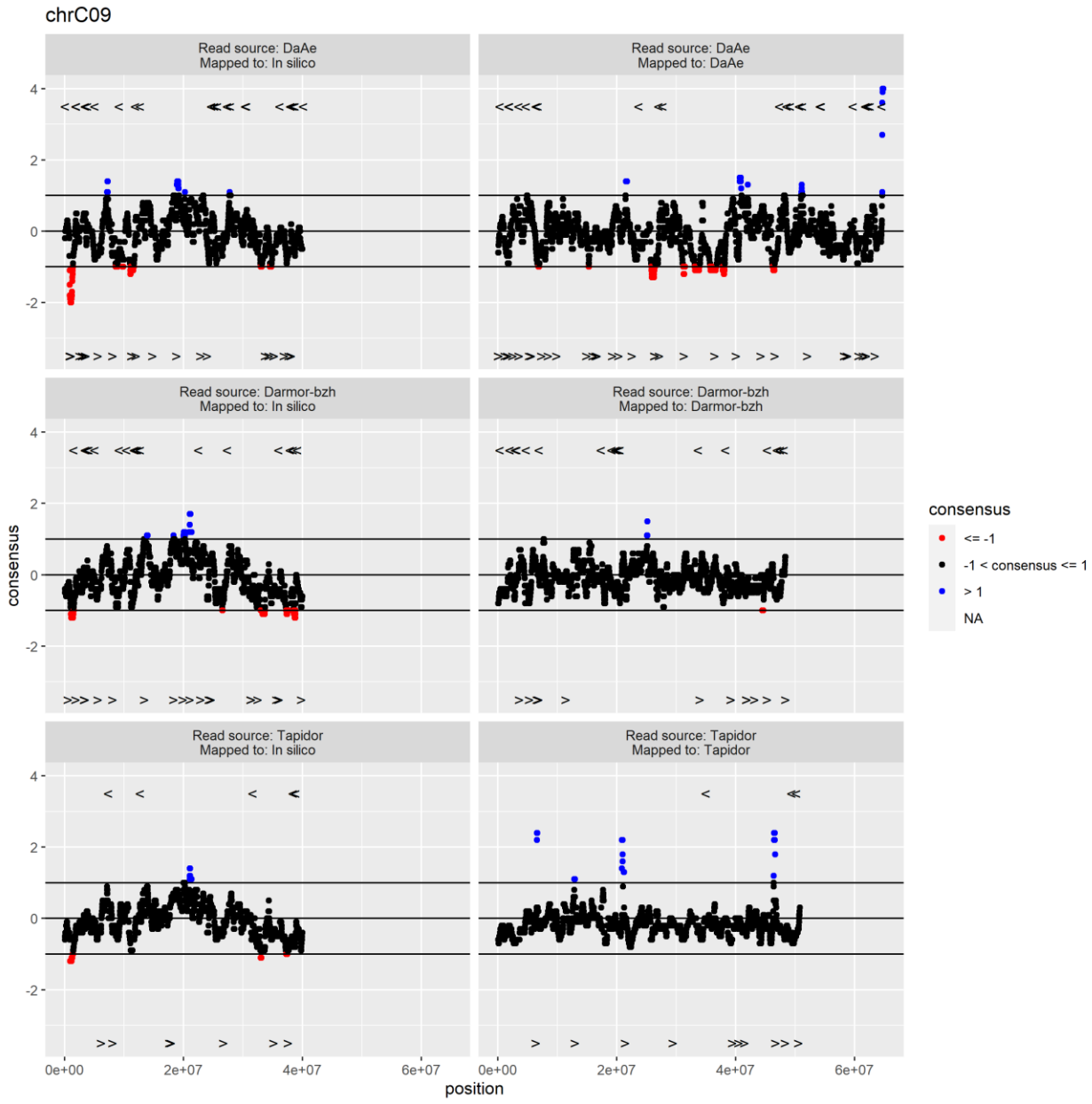

Supplementary Figure 19 Coverage of each genome. "<" indicates recipient and ">" indicates donor locations of genes suspected to be involved in homoeologous exchange.

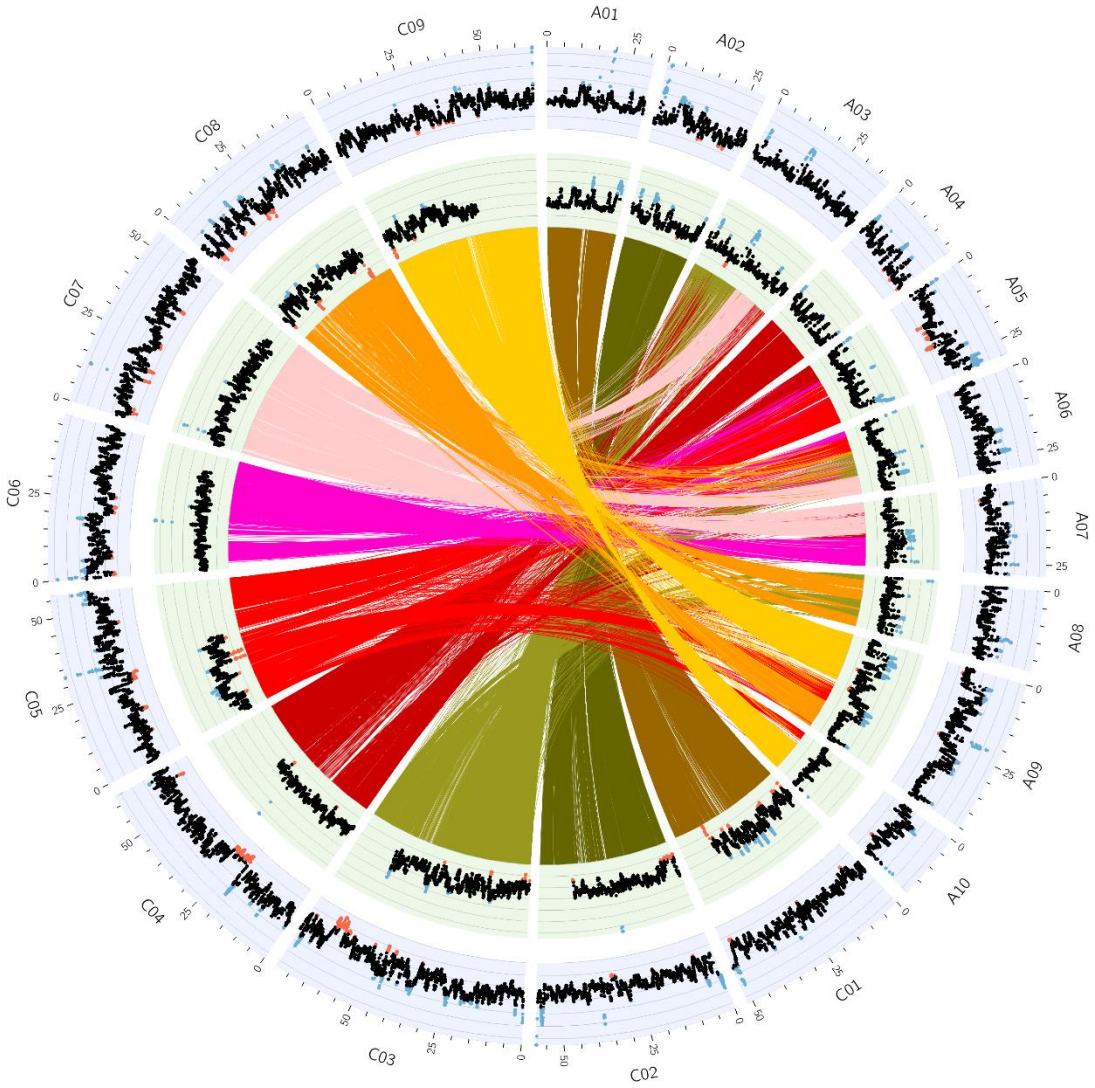

Supplementary Figure 20 Circos plot of Da-Ae. Outer blue track is read coverage across the Da-Ae genome. Inner green track is read coverage across the in silico genome (B. rapa + B. oleracea). Blue dots indicate standardized coverage greater than 1 and red dots indicate standardized coverage less than -1. Ribbons in the center of the plot indicate regions of homology between the A and C subgenomes. Colors have been assigned based on C subgenome chromosomes.

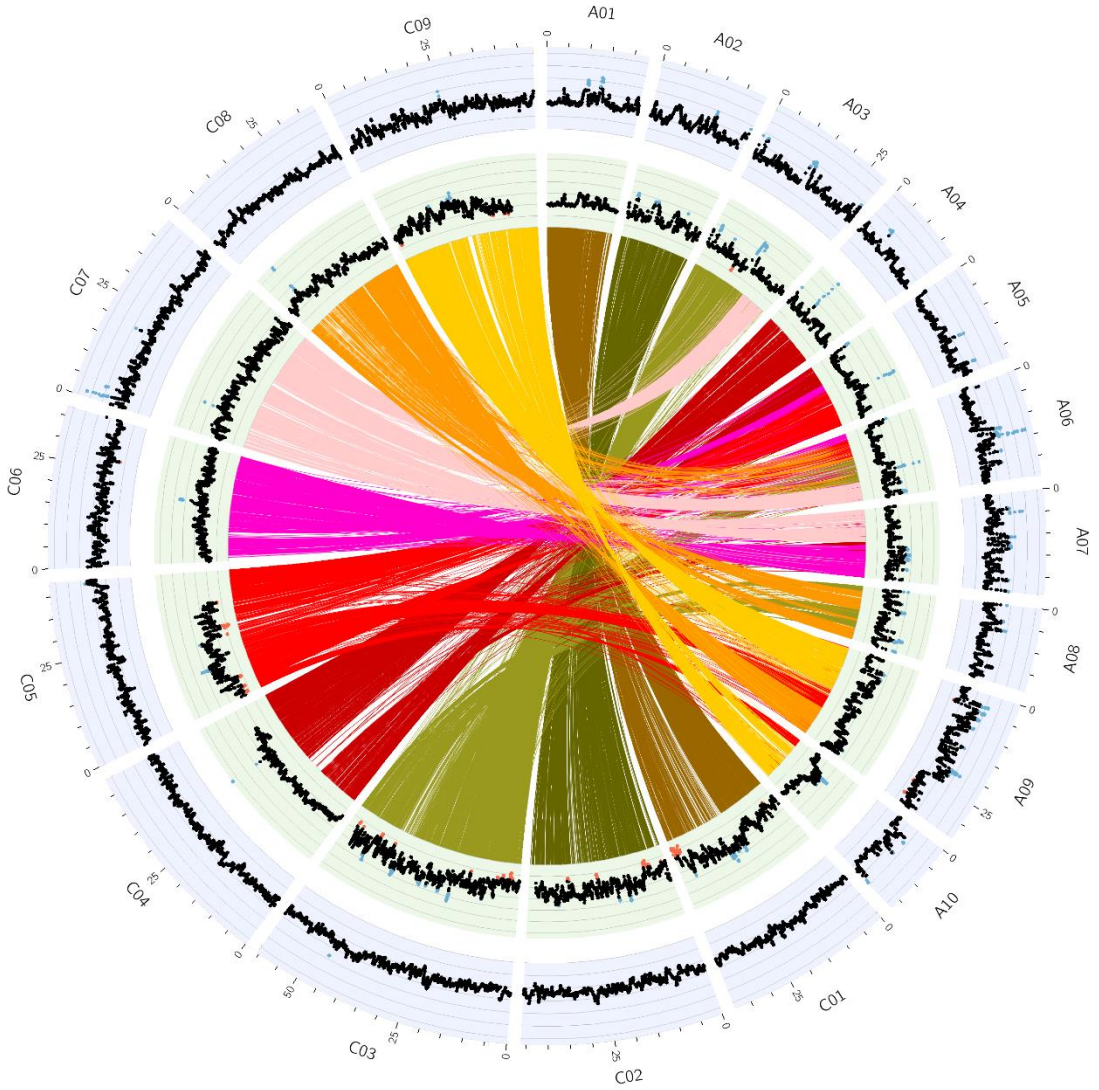

Supplementary Figure 21 Circos plot of Darmor-bzh. Outer blue track is read coverage across the Da-Ae genome. Inner green track is read coverage across the in silico genome (B. rapa + B. oleracea). Blue dots indicate standardized coverage greater than 1 and red dots indicate standardized coverage less than -1. Ribbons in the center of the plot indicate regions of homology between the A and C subgenomes. Colors have been assigned based on C subgenome chromosomes.

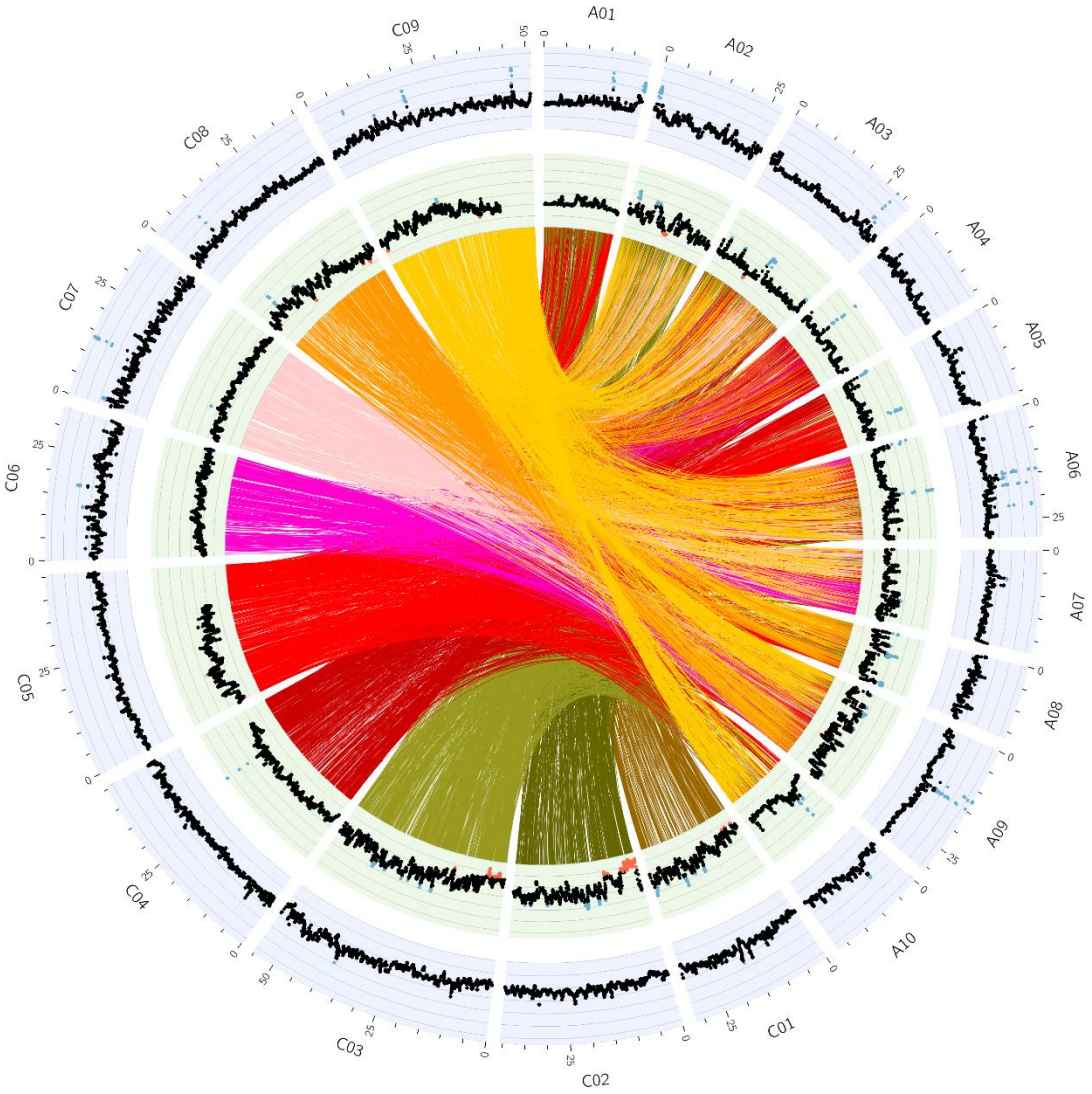

Supplementary Figure 22 Circos plot of Tapidor. Outer blue track is read coverage across the Da-Ae genome. Inner green track is read coverage across the in silico genome (B. rapa + B. oleracea). Blue dots indicate standardized coverage greater than 1 and red dots indicate standardized coverage less than -1. Ribbons in the center of the plot indicate regions of homology between the A and C subgenomes. Colors have been assigned based on C subgenome chromosomes.

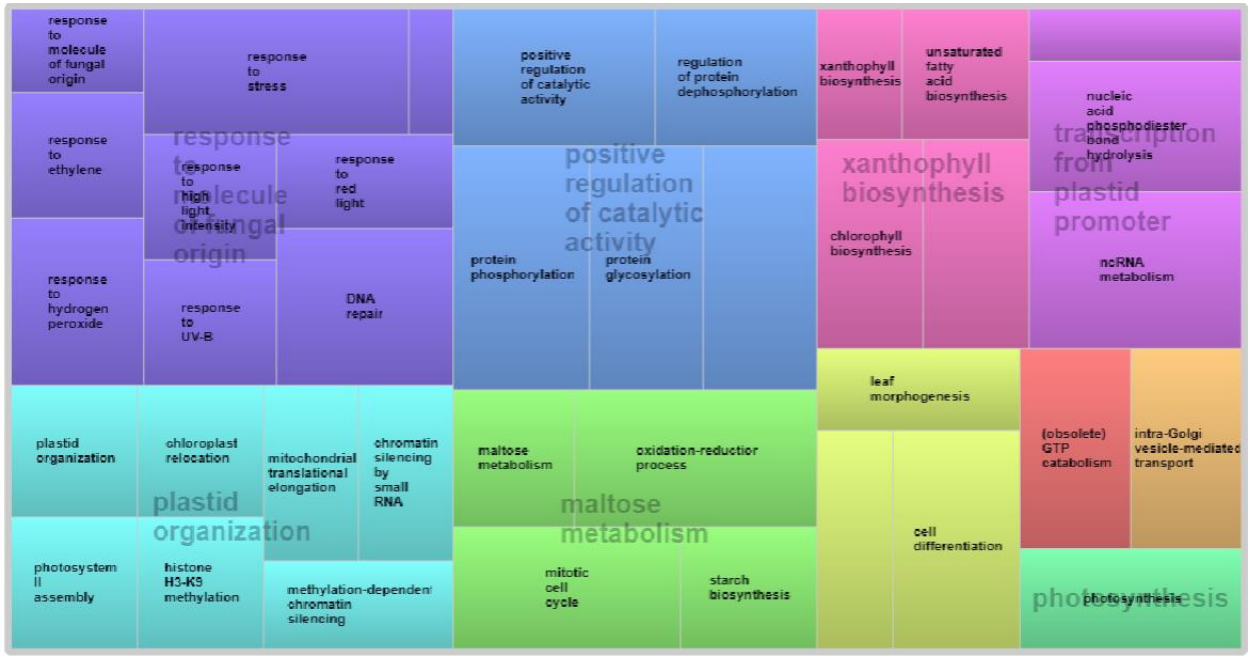

Supplementary Figure 23 Revigo results for Biological Processes connected to the shared single copy BUSCOs

Supplementary Tables

Supplemental Table 1 Discrepancies between Da-Ae and Darmor-bzh assemblies. Discrepancy number, chromosome discrepancy is located on, type of discrepancy, data able to support Da-Ae's composition, and action taken to resolve discrepancy.

Discrepancy	Chromosome	Type	Supported	Action taken
1	A01	Inversion	Yes	None
2	A02	Inversion	No	Flipped
3	A02	Duplication	Yes	None
4	A03	Inversion	No	Flipped
5	A04	Inversion	Yes	None
6	A05	Inversion	No	Flipped
7	A06	Inversion	Yes	None
8	A07	Inversion	Yes	None
9	A08	Inversion	Yes	None
10	A09	Gap	Yes	None
11	A10	Inversion	Yes	None
12	C01	Inversion	No	Flipped
13	C02	Inversion	Yes	None
14	C03	Inversion	No	Flipped
15	C04	Inversion	Yes	None
16	C05	Inversion	No	Flipped
17	C05	Inversion	Yes	None
18	C06	Inversion and Gap	No	Flipped and Joined
19	C06	Inversion	No	Flipped
20	C06	Inversion	Yes	None
21	C07	Gap	No	Joined
22	C07	Inversion	Yes	None
23	C08	Duplication	Yes	None
24	C09	Inversion	Yes	None